Marine and Petroleum Geology 114 (2020) 104242

Contents lists available at ScienceDirect

Marine and Petroleum Geology

journal homepage: www.elsevier.com/locate/marpetgeo

Research paper

Orogen-transverse structures in the eastern Himalaya: Dextral Riedel shear along the Main Boundary Thrust in the Garu-Gensi area (Arunachal Pradesh, India), implication in hydrocarbon geoscience

Tapos Kumar Goswami[a], Bashab Nandan Mahanta[b], Soumyajit Mukherjee[c,*], Banteilang Rapthap Syngai[d], Ranjan Kumar Sarmah[a]

[a] Dept. of Applied Geology, Dibrugarh University, Dibrugarh, 786004, Assam, India
[b] Geological Survey of India, Shillong, 93003, Meghalaya, India
[c] Department of Earth Sciences, Indian Institute of Technology Bombay, Powai, Mumbai, 400 076, Maharashtra, India
[d] Geological Survey of India, Kokata, West Bengal, India

ARTICLE INFO

Keywords:
Collisional orogen
Shear zone kinematics
Seismicity
Petroleum geology

ABSTRACT

Structural mapping and analyses reveal deformation in the rocks of the Lesser Himalayan Miri and Gondwana, and Lower Siwalik Dafla successions across the Miri Thrust (MT) and the Main Boundary Thrust (MBT) in the Garu-Gensi area (Arunachal Himalaya, India). The-north-dipping Gondwana sequence is sandwiched between the Miri Group of rocks in the north and the Lower Siwalik Dafla sandstones in the south. The Gondwana rocks folded four times (D_1-D_4). Detail outcrop mapping and structural analyses substantiated by satellite images elucidate that the Miri, the Gondwana and the Lower Siwalik rock sequences in the area are traversed by two sets of NW and NE trending cross-fault zones with~70–100 m thickness mappable for ~70 km. The cross-faults trend NW around the locality Daring, while in the western part around Gensi, they trend NE. The westernmost fault slipped dextrally and the easternmost one at Daring sinistrally. These transverse faults offset the MBT: 0.52–0.59 km for the western- and 0.58–1.41 km for the eastern faults. The deformation in the Gondwana sequence may be constrained as syn-Himalayan (i.e., India-Asia collisional event). This was followed by a compression from E/ESE due to the post-Eocene Indo-Burmese collision. The culminating phase of combined India-Asia and Indo-Burmese compression is manifested in field with a strong NE-directed compression with dextral Reidal shear developing in the transverse conjugate fault zones in the area with maximum displacement towards SE. Cluster of the earthquake data indicates record of the events (M ≥ 6) within 30–80 km depth-both N and S of the MBT in the study area. Further, the southerly continuation of the transverse faults below the alluvium can provide vital clue in studying the potential hydrocarbon trap in the northern fringe of the Brahmaputra river.

1. Introduction

The Himalayan mountain belt is a classic example of the continent-continent collision since ~ 54 Ma (Yin, 2006; Hu et al., 2016; Najman et al. 2017). It is characterized by longitudinally extensive collisional fold-thrust belts. Towards north, the Himalaya is divided into Sub-Himalayan Siwalik sequence, the Lesser Himalaya, the Higher- or the Greater Himalaya and the Tethyan Himalaya (Yin, 2006; Mukherjee, 2015; Bose and Mukherjee, 2019a,b). Their bounding faults northward are the Himalayan Frontal Thrust (HFT) or the Main Frontal Thrust (MFT), the Main Boundary Thrust (MBT), the Main Central Thrust (MCT) and the South Tibet Detachment (STD), respectively (Fig. 1a). In the eastern Himalaya, the MBT separates the Lesser Himalayan Gondwana rocks from the Neogene sub-Himalayan Siwalik sequences (Bose and Mukherjee, 2019a,b).

The multiple-deformed Lesser Himalayan rocks are reported from several portions of the orogen, e.g., Tansen–Pokhrara section in the Central Nepal (five phases: D1-D5; Paudel and Arita, 2000), north of the

Abbreviations: AH, Arunachal Himalaya; BF, Banderdewa Fault; BM, Bomte Member; HFT, Himalayan Frontal Thrust; LG, Lower Gondwana; LHD, Lesser Himalayan Duplex; MFT, Main Frontal Thrust; MBT, Main Boundary Thrust; MCT, Main Central Thrust; MDZ, Main Deformation Zone; MQ, Miri Quartzite; MT, Miri Thrust; MTS, Miri Thrust Sheet; RM, Rilu Member; STD, South Tibet Detachment

* Corresponding author.
E-mail addresses: soumyajitm@gmail.com, smukherjee@iitb.ac.in (S. Mukherjee).

https://doi.org/10.1016/j.marpetgeo.2020.104242
Received 22 May 2019; Received in revised form 28 December 2019; Accepted 13 January 2020
Available online 18 January 2020

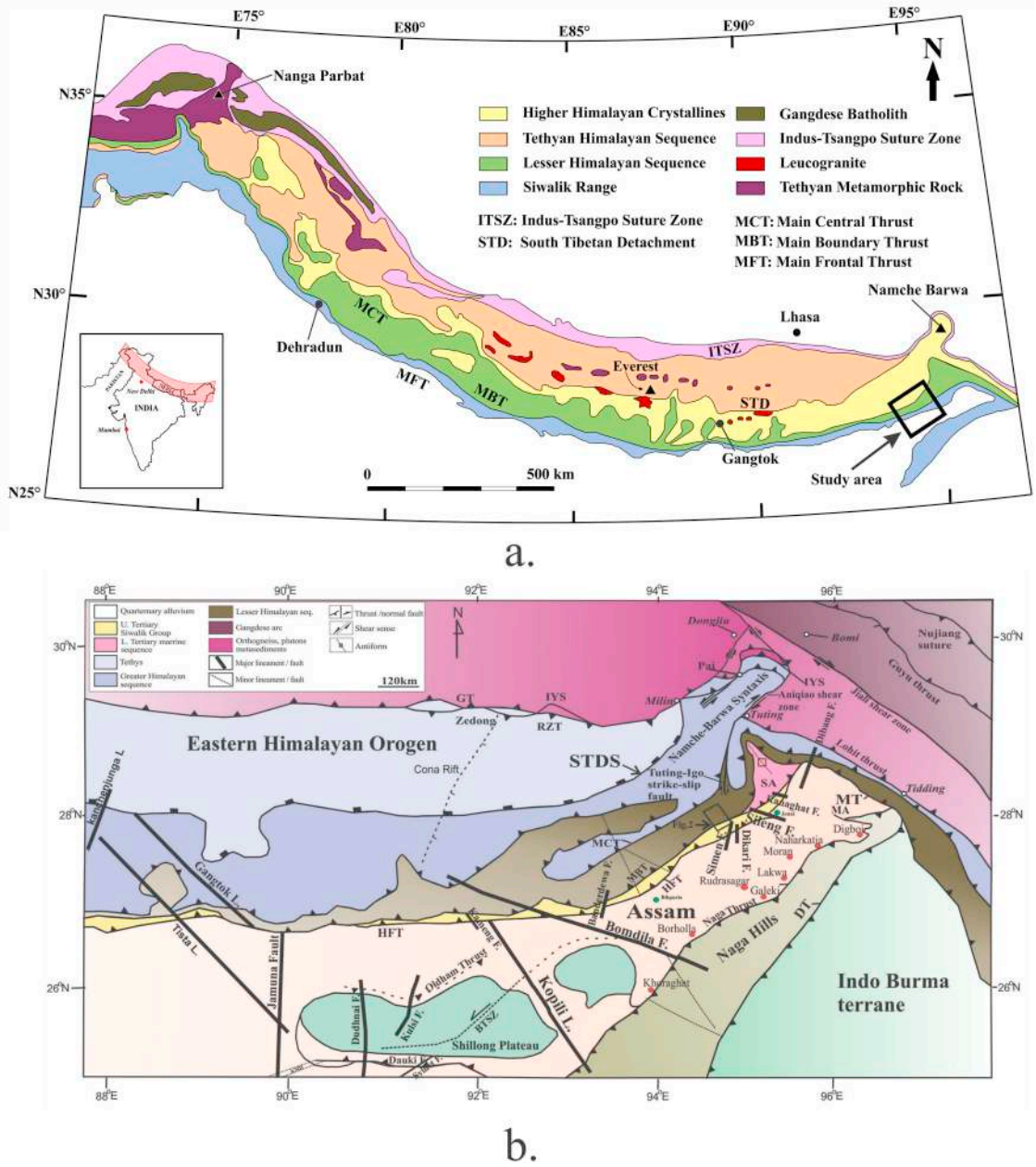

Fig. 1. aGeological map of Himalayan orogen (modified after Yin et al., 2010) showing the locations of Arunachal Himalaya. The study area is shown by a black rectangle. b. Regional geological sketch map of eastern Himalayan Namche Barwa syntaxis and adjoining regions (modified after Ding et al., 2001). Area of study across MBT marked with bold rectangle. Jiali and Pai shear zones (with opposite shear senses) flank the Namche Barwa syntaxis. Lohit Thrust is truncated against Aniqiao shear zone (north of Tuting) which is connected to Tuting-Igo strike-slip fault. Kanchenjunga, Tista and Gangtok Lineaments (Dasgupta et al., 2013); Jamuna, Sylhet, Dauki and Kopili Faults and minor lineaments (Mukhopadhyay, 1984); Dudhnoi and Kulshi Fault (Duarah and Phukan, 2013); Bomdila Fault (Kayal et al., 1993; Sarma and Sharma, 2018). Solid red circles indicate oil fields of Upper Assam shelf (Palaeogene and Neogene sequences (Dasgupta and Biswas, 2000). The green solid circle in the north indicates potential area in consideration of oil exploration (Ghosh et al., 2010). GT: Gangdese Thrust, IYS: Indus Yalu Suture, RZT: Renbu Zedong Thrust, STDS: South Tibet Detachment System, MCT: Main Central Thrust, MBT: Main Boundary Thrust, HFT: Himalayan Frontal Thrust, NT: Naga Thrust, MT: Mishmi Thrust, DT: Dishang Thrust, SA: Siang Antiform. Locations of oil well in the Brahmaputra valley are shown by red filled circles. In the northern part of Brahmaputra, the drilling operations are in Jonai and Bihpuria (green filled circles). (For interpretation of the references to colour in this figure legend, the reader is referred to the Web version of this article.)

Ramgarh Thrust in Sikkim Himalaya (single phase: D_1 with six stages: A-E; Matin and Mukul, 2010), fore- and back-thrusts from the Garhwal (Bose and Mukherjee, 2019a; see Jayangondaperumal et al., 2018 for other details) and the Sikkim Himalaya (Bose and Mukherjee, 2019b); and the Bomdila-Zimithang area of the western and Daporijo-Yapuik region of the eastern Arunachal Himalaya (three Phases: D_1-D_3,Schelling and Arita, 1991; DeCelles et al., 2002; Bhattacharya and Nandy, 2007; Srivastava et al., 2011; Singh and Gururajan, 2011; Sarma et al., 2014; Saha, 2013; Matin and Mazumdar, 2009). Focused erosion seems not to be a guiding factor for the Himalayan orogeny in the Arunachal sector (Adlakha et al., 2019). The Himalayan orogen, and especially the Lesser Himalaya, is characterized by several transverse features that separate the mountain ranges into different thicknesses of sedimentary units and deformation styles (Valdiya, 1980a; Godin and Harris, 2014; Godin et al., 2019). Lateral variation in tectonics in the Himalaya is also linked with the lateral ramps along the main thrusts (Wu et al., 1998).

Further, the Precambrian basement ridges (Delhi-Hardwar ridge,

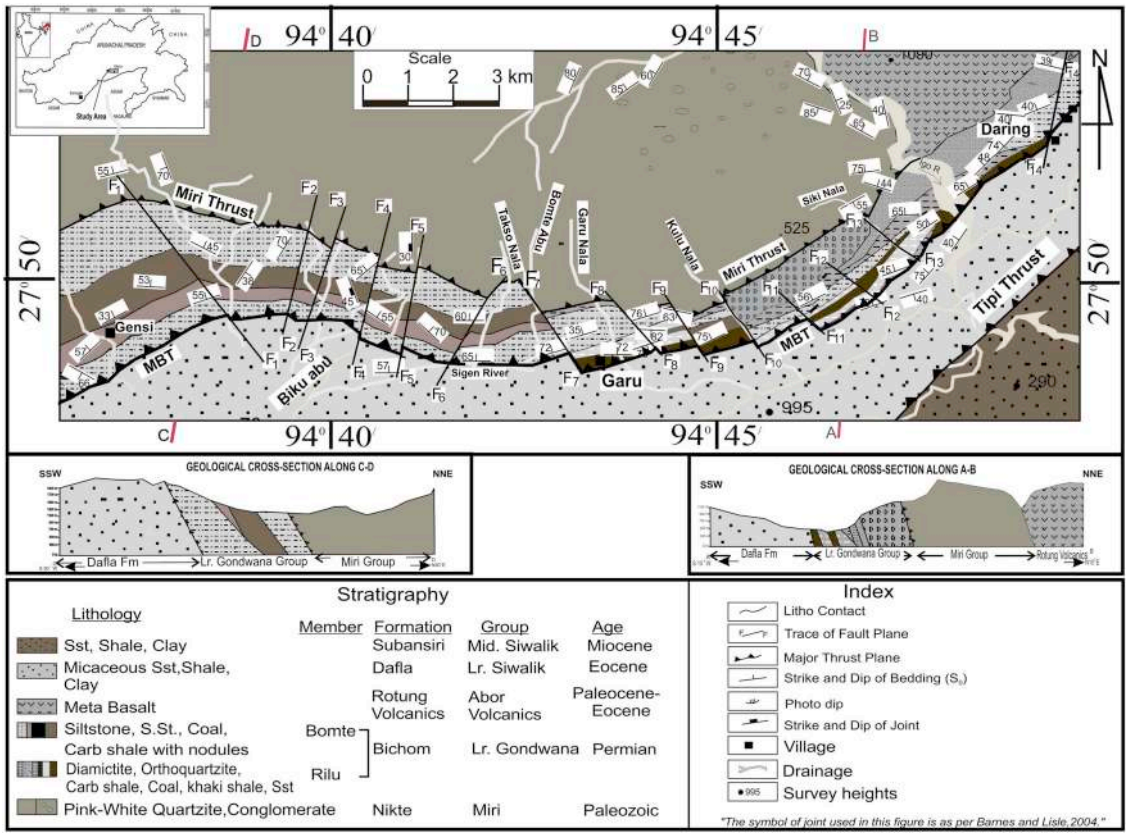

Fig. 2. Geological map (prepared by these authors) of the Daring-Garu-Gensi area, West. Siang and East Siang Districts, Arunachal Pradesh (Inset: Location map of the area studied). The two fault zones in the eastern and western part of the study area (excepting two faults) Trend NW and NE. Unbalanced Cross-sections along AB and CD are shown below. These are prepared by the authors themselves based on their fieldwork. Lithotectonic sequence from Palaeozoic to Miocene exposed in the area in the inset.

Faizabad ridge, Munger-Saharsa ridge) and the major faults such as the Great Boundary Fault, Lucknow Fault, Son-Narmada Fault, Pingla Fault, the Eocene hinge zone, and the Dhubri Fault beneath the Ganga and the Brahmaputra alluvial plains trend high-angle to the strike of the Himalaya (Godin and Harris, 2014 and their Fig. 2a). These structures also continue beneath the E-W trending Himalayan orogen (referred in Godin et al., 2019; Bose and Mukherjee, 2019a,b). These ridges may either be the fault-bound margins of the north Indian craton or are the Gondwana failed rifts produced due to tectonic extension (Prasad and Rao, 2006; Bhattacharyya and Mitra, 2009). As the Indian plate has been underplating below the southern Tibet (/the Lhasa block), few of the basement faults south of the Himalayan front remain seismogenic (Godin et al., 2019). A number of transverse faults or high-strain zones with the Paleoproterozoic sedimentary basin fills are mapped in the foreland of the Himalayan orogen in the northern Indian craton (Martin, 2017). The offset of the Main Boundary Thrust (MBT) due to lateral/oblique ramping has been deciphered in the western and in the central Himalaya (Shah et al., 2012; Dubey, 2014).

This work presents the deformation style in the Miri–Gondwana–Siwalik sequence in the transverse fault zones along the MBT in the Garo-Gensi of the eastern Arunachal Himalaya (AH). The study reports deformation in the Gondwana rocks and its regional implication, and the nature of the thrust contacts at N and S. We also report ~70–100 m thick fourteen fault zones (eight out of which trend NW) in the study area mostly consists of sandstones and shales. Together with the MT and the MBT, they can provide crucial information on how regional brittle faults activate in a collisional orogen (Holdsworth et al, 2002; Jones et al., 2004). Further, the work also draws attention in regard to studying southerly continuation of the transverse faults in the search of potential hydrocarbon accumulation in the north Brahmaputra basin.

2. Orogen-transverse faults in the eastern Himalaya

The manifestation of the complex interaction of the Himalayan and Burmese collision orogen at N and E are revealed in the eastern Himalaya and in its foredeep in terms of a number of prominent orogen-transverse lineaments and faults. Some of these lineaments continue even into the Bengal basin by extending through the Himalayan foredeep for hundreds of km (Mukhopadhyay, 1984; Roy and Chatterjee, 2015; Hossain et al., 2019). A number of these cross-structures are the pre-Himalayan basement faults that subsequently underplated below the Himalayan orogenic wedge (Godin and Harris, 2014). Conjugate strike-slip faults such as the NNE trending Kanchenjunga lineament, and the NNW trending Tista and Gangtok lineaments indicate tectonic inhomogeneity in the Himalayan front (Dasgupta et al., 2013). East of the Tista lineament, the N–S trending Jamuna/Dhubri Fault outlines the western margin of the Shillong plateau (Fig. 1b; Table-1).

In the AH, segmentation of MBT by deep-seated strike-slip faults is presumably a major cause of the 50–80 km deep micro-seismicity (Kayal, 2001). The controlling factor for the along-strike sinuosity of the mountain front and segmentation in seismicity may be attributed to the transverse faults (Bhakuni et al., 2017 and references therein).

Within the Shillong plateau, two major basement faults: the NNE trending Kulsi Fault and the N trending Dudhnoi Fault account for the major present day seismicity (Duarah and Phukan, 2013). In the western Assam, traversing HFT along Manas and Dhansiri Rivers, the frontal fault scarps are associated with the NNW facing back-scarps (Pandey et al., 2018). The offset in the HFT and the Tipi Thrust (TT) in the western AHarelinked to the movement along the NNW trending

Kameng Fault (Fig. 1b; Srivastava and Misra, 2008; Goswami et al., 2018). Along this section, two strands of the HFT, the HFT-1 and the HFT-2, define a small intermontane valley in between. The Kameng river flows along this valley. The HFT-1 is intersected by a number of tear faults trending N–S to NE-SW for~ 1–2 km (De Sarkar et al., 2014). HFT-2 deflects around the Balipara anticline (Yin et al., 2010; De Sarkar et al., 2014) and merge with the HFT-1 at SE.

The NNW trending Kopili Lineament (the Kopili valley itself), between the Shillong Plateau and the Mikir massif, is seismically active (Srivastava et al., 2013). The Kopili lineament extends from the AH in the north through the Kopili valley to the Naga schuppen zone (Mukhopadhyay, 1984). Juxtaposed to east of the Kopili Lineament, the NNW trending Bomdila Fault also extends from the AH into the Naga schuppen zone (Sarma and Sharma, 2018). In the Dikrong river valley of the Central AH, along the HFT, ~ 10 km offset in the mountain front is calculated through sudden widening of the Dikrong river channel along a NW trending transverse Banderdewa Fault (BF) between the locations Banderdewa and Gumtu (Devi et al., 2010). Moreover, in the eastern AH, the offset in the mountain front, distorted channel pattern and terrace uplift are related to number of orogen-transverse faults, which segmented the HFT and the MBT (Bhakuni et al., 2017). These are: *(i)* NE trending Simen fault along the Simen river, *(ii)* NNW trending Dikari fault along the Dikari river, *(iii)* WNW trending Sileng Fault along the Sileng river, *(iv)* NW trending Ranaghat fault along the Siang river. Further, the Mishmi Thrust and the MBT are segmented by a NNE trending Dibang Fault along the Dibang river (Bhakuni et al., 2017). The N-trending Tuting-Bame Fault or the Tuting-Igo Fault is a major dextral fault in the left limb of the Siang antiform (Nandy, 1980; Kumar, 1997).

In the easternmost AH, the Mishmi Thrust trends NW (Mishra, 2009; Sarma et al., 2017; Ningthoujam et al., 2015). The NW trending axial traces of the Manabum- and the Siang antiforms (Fig. 1b) are also highly oblique to the general trend of the AH. The along-strike crustal shortening of the orogeny (Dutta et al., 2019), such as in the eastern Himalaya has been substantially accommodated by these transverse faults (Hazarika et al, 2010; Dasgupta et al., 2013). Further, in the eastern limb of the Siang Antiform or in the eastern flank of the eastern Himalayan orogen, a greater degree of underthrusting of the Indian craton rocks is reported compared to Himalayan orogen in the west (Haproff et al., 2019).

3. Geology of the study area

In the AH, the Lesser Himalayan Gondwana rocks are bound by the MBT in the south and the Miri Thrust (MT) in the north. The study area is located in the southwestern part of the Siang Antiform in the eastern AH (Fig. 1). The area covers ~225 km^2 and is located in the East and West Siang Districts of the Indian state Arunachal Pradesh. Towards north, the Miri Group of Lower Palaeozoic rocks juxtapose with the outer Lesser Himalayan phyllite-quartzite sequence along the Bomdila Thrust (Singh and Gururajan, 2011). The Ramgarh Thrust in the Darjeeling-Sikkim Himalaya (~800 km east from the study area) underlies the Daling, the Buxa, and the Gondwana rocks and constitutes the Lesser Himalayan Duplex (LHD; Matin and Mazumdar, 2009; Bose and Mukherjee, 2019b). The Ramgarh Thrust sheet overlies the Proterozoic Daling sequence in the Sikkim Himalaya (Matin and Mazumdar, 2009 and references therein); . This thrust sheet in other parts of the Himalaya has the similar structural position in the footwall of the MCT (Mullick and Basu Chowdhury, 1966; Valdiya, 1980a; Srivastava and Mitra, 1994; DeCelles et al., 2002; Mukherjee, 2015; Pearson and DeCelles, 2005). Thus, The MT, like the Ramgarh Thrust, transports a similar sequence of Proterozoic pelitic sequence in the hangingwall with respect to the Gondwana sequence in the footwall (Fig. 2). The MT also correlates with the North Kalijhora Thrust in the Darjeeling–Sikkim Himalaya and the Shumar Thrust in Bhutan Himalaya (McQuarrie et al., 2008), which was re-designated by Mukherjee (2015) as an out-of-sequence thrust having made this regional correlation.

The deformation of the Lesser Himalayan sequence in the Sikkim-Bhutan and the AH has been studied and reviewed by several workers (Gangopadhyay and Ray, 1980; Singh et al., 1983; Ray et al., 1989; Bhusan et al., 1991; Ray, 1995, Kumar 1997; Mukul, 2000; Yin, 2006; Bhattacharya and Nandy, 2007; Goswami et al., 2009; Matin and Mazumdar, 2009; Mitra and Bhattacharyya, 2011; Saha et al., 2011; Srivastava et al., 2011; Saha, 2013; Bhattacharyya et al., 2015a, b; Pauri and Bhattacharyya, 2018; Chakraborty and Mukul, 2019). However, the deformational imprints in the Gondwana sequence (= "Supersequence VI" of Kumar, 1997) and the nature of the thrust contact of the Gondwana sequence with the MT in the north and MBT in the south remain poorly studied. Additionally, rocks of the Gondwana sequence within the two major thrusts deformed repeatedly (Singh et al., 1983; Singh and Chowdhury, 1990).

The Lower Palaeozoic Miri Group (Kesari, 2010), in the hangingwall of the Miri Thrust (MT), is in the north of the Gondwana sequence. The Middle Miocene Lower Siwalik Dafla Formation occurs in the footwall of the MBT at its S (Fig. 2). The Gondwana rocks of the area represent the litho-tectonic units equivalent to the Ranjit Pebble Slate (Acharyya et al., 1975; Acharyya and Ray, 1977) with basal Gondwana diamictites and associated sedimentary succession of the Early to Late Permian marine and lagoonal environments. The lithounits occur as thrust slices with both vertical and lateral facies variations (Kumar and Singh, 1974; Roy Chowhury, 1978; Tripathi and Roy Chowdhury, 1983; Singh, 1981). The Siwaliks, S to the MBT, represents a fluvial facies. In the AH, the Gondwana rocks deposited along E-W to ENE-WSW narrow and linear belt for ~ 300 km and constitute a lithological and faunal facies change from continental in the W of Dikrong river to marine from Dikrong to Pashighat (Tripathi and Roy Chowdhury, 1983). From Bhutan in the W to the Dikrong river section in the Lower Subansiri District in the E, the continental Gondwana rocks crop out while in the E of Dikrong river, the marine Gondwana rocks occur. The exact nature of the contact, between the continental and the marine Gondwana rock, whether tectonic or atectonic, has remained indeterminate.

4. Present works & discussions: transverse faults in the study area

4.1. Mapping

The Miri, the Gondwana and the Siwalik rocks in the study area are segmented by several NW and NE trending transverse faults. The concisestraigraphy of the area is presentedin Fig. 2. The detail stratigraphy of the area is presented as the Repository Table 1. The fault contact is between the Palaeozoic Miri Group and the Permian Lower Gondwana sequences along the MT. The Lower Gondwana (LG) Bichom Formation is divided into the Lower Rilu Member (RM) and the Upper Bomte Member (BM). These faults are identified by the along-strike termination of the rocks against different lithologies documented in the nala (small water flow) sections.

The lithologic discontinuity along the MBT zone along-strike is mapped on ground and using Google Earth images in this work for ~70 km. Table 2 presents the terminations of lithology across each fault. The western faults (Fault 1 to 6; the known nala sections are the Biku Abu: Fault F2 and the Sigen nala: Fault-6; the names of the other nala sections are not known to the local villagers) trend between N38°W to N29°E. The faults dip 84° due NE to 86° due NW directions. The Lower Gondwana (LG) sequence is folded and the siltstone bed of the BM appear both in the N and Sto the west of Takso Fault. Further, the Lower unit of the LG, the Rilu Member (RM) disappears in the W of the Takso Fault.

Among the NE-trending western faults (F1–F6), along the Biku Abu fault and other faults (F1, F3–F5), the abrupt terminations of the siltstones of the BM against the Miri Quartzite (MQ) in the north, and Dafla sandstone in the south are recorded (Figs. 2 and 3). Further north, termination of siltstone of BM against MQ is mapped for ~ 0.41 km. In

Table 1
Orogen transverse faults and lineaments in eastern Himalaya.

Fault/lineament/window/anticline	Extension	Trend	Record of seismicity	References
Kanchenjunga L	Towards NE, across Lesser and Higher Himalaya; towards SW, Himalayan foredeep	NNE	Yes	Dasgupta et al. (1987); Dasgupta et al. (2013);
Tista L	Towards NW, across Lesser and Higher Himalaya; towards SE, Himalayan foredeep	NNW	Yes	Mukhopadhyay, 1984; Dasgupta et al. (2013); Roy and Chatterjee, 2015
Gangtok L	Sympathetic to TL; towards NW across Higher Himalaya; towards SE within Lesser Himalaya	NNW	Yes	Mukhopadhyay, 1984; Dasgupta et al. (2013);
Jamuna F/Dhubri F	Western margin of the Shillong Plateau	NS		Duarah and Phukan, 2013;
Kulshi F	Within the Shillong plateaau	NNE	Yes	Duarah and Phukan, 2013
Dudhnoi F	Basement fault within the Shilling Plateau	NS	Yes	Duarah and Phukan, 2013
Kameng F	Towards NNW across sub- Himalayan Siwalik belt in western Arunachal Himalaya towards SSE Brahmaputra alluvium	NNW		Srivastava and Misra, 2008; De Sarkar et al. (2014); Goswami et al. (2018);
Kopili Lineament	Between Shillong Plateau and Mikir Massif; towards NNW across Lesser and Higher Himalaya; towards SSE within Naga Schuppen zone	NNW	Yes	Kayal (2001), 2006; 2008
Bomdila F	Towards NW across Lesser and Higher Himalaya; towards SSE extended up to Naga-Dishang Thrusts.	NW	Yes	Murty, 1983; Nandy, 1980; Kayal, 2001; Sarma and Sharma (2018).
Dikrong F	Towards NNW Lesser Himalaya; towards SSE extended up to Brahmaputra alluvium	NNW	Yes	R K M Devi et al., 2010; Mishra, 2009
Simen F	Displaced Sub Himalayan Siwalik sequence	NNE	Yes	Bhakuni et al. (2017)
Dikari F	Displaced Himalayan Siwalik sequence	NNW	Yes	Bhakuni et al. (2017)
Sileng F	Displaced Himalayan Siwalik sequence	WNW	Yes	Bhakuni et al. (2017)
Tuting-Igo F	Across Higher and lesser Himalaya	NS	Yes	Nandy, (1980); Kumar, 1997
Ranaghat Fault	Across Lesser Himalaya and Sub Himalaya	NW	Yes	Bhakuni et al. (2017)
Dibang Fault	Across lesser Himalaya and Higher Himalaya	NE	Yes	Bhakuni et al. (2017)
Siang antiform/Siang Fracture	Across MBT/NPT transgressing Lesser and Higher Himalaya	NNW	Yes	Acharyya (2015)
Manabum antiform	Across Naga thrust	NNW	Yes	Acharyya (1980) Acharyya (2015)

the NW-SE trending eastern faults (F7–F14), an abrupt termination of the orthoquartzite against the Lower Gondwana carbonaceous shale (Rilu Member: RM) is observed west of the Siki Fault (F12) (Fig. 2). Along the Kulu Fault, the khaki (brownish-yellow)shale-sandstone-carbonaceous shale succession terminates against the diamictite layer. The shale-carbonaceous sequence along the Garu Fault, identified by us, terminates against the Miri Quartzite (Figs. 2 and 3). On the other hand, the carbonaceous shale of the Rilu Member (RM) that terminates against the sandstones of the BM is mapped as the Kulu Fault. We have also recorded that in all the western faults (west to the Takso Fault), within BM, the sandstones terminate against the siltstones (Figs. 2 and 3).

Mapping conducted on a topo-sheet of 1:25,000for the different lithologic units- Miri, Gondwana and Lower Siwalik Dafla along the MBT zone indicates that the slip magnitude varies amongst the different fault zones. The fault slip data (dip and dip directions of faults, lithologies across, slip magnitude and sense) along the Miri- Gondwana contact and the Gondwana –Lower Siwalik contact are presented in Table 2. Out of the total 14 slip data for faults, names of the some of the nala sections are stated in the table. The range of slip along the MBT measured in the field and also on the image is 0.02–0.925 km. As per Fig. 2, the measured slips along the faults are: for the westernmost NW-SE fault (F1) is 20 m when measured along the Gondwana –Miri contact. From Daring to Gensi for ~ 70 km, the offsets in the MBT are mapped showing local increase in slip magnitude towards ENE. The maximum slip of0.93 km is noted along the Takso nala (Fig. 2; Table-2).

To determine the amount of slip across the MBT and the MT, we measured the corresponding termination of the lithologic units along-strike in different fault zones. Eight faults, viz., Takso to Siki Nalas (Figs. 2 and 3) trend NW. These faults are considered as the Group-1 faults. Five faults west of the Sigen river trending NE (Figs. 2 and 3) are considered as the Group–2 faults. The grouping is based on the spatial occurrence and the trend of the fault zones: the Group-1 faults trend NW and the Group 2 faults NE. Faults reported in this study do not show drag folds of the layered rocks near them. None of the faults reported are the back thrusts (i.e., thrusts with ~ N vergence).

5. Transverse faults across the MT

The MT brings the Lower Palaeozoic Miri Group of rocks (Miri Thrust Sheet) above the Permian LG sequences of the Bichom Formation (Figs. 2 and 3). The MQ-LG contact is mapped from Daring to Gensi along an E-W traverse for ~60 km. The extent of the vertical exposures of the lithologic discontinuity for all the nala sections ranges 70–100 m.The general trend of the Miri Group of rocks in the western part of the study area is NE (52°)with moderate to steep dips (31-64°) towards north. In the eastern part of the area, the beds are steeper (59-79°) with trendsvarying309° to 69° (Fig. 3). The foliated Miri quartzite dips steeply near the thrust contact with the Lower Gondwana sandstone-shale-phyllite sequence.

Mesoscopic antiforms and synforms are observed in the Miri quartzites, in the north of Siki nala. The axial planes of the antiform and synform dip 72° and 71°, respectively towards NW (Fig. 3b and c; 4a,b). The beds are usually sub-vertical with very steep dip towards N (Fig. 4c). Miri quartzites and shales with sub-vertical beds also exist along the Takso nala section (Fig. 4d). Sigmoid lenses in the shale bed shows a SW-directed foreland vergent shear. Fig. 5apresents a top-to-SW shear in the Miri quartzite. The same shear sense in the Miri quartzite is also recorded in the Takso nala (Fig. 5b), and along the Miri Thrust in the Siki nala, Takso nala and the Biko-Abu nala sections.

Remarkably, along the Garu-Rilu road, folded Gondwana sandstones in the thrust contact are back folded (i.e., vergeing towards NE) with NW-SE trending axial plane dipping ~ 65° (Fig. 5c). At the Bomte nala, the asymmetric sigmoid slivers of the Miri quartzite within the grey shale beds of Gondwana preserve a top-to-SE shear (Fig. 5d). The shear foliation (C) and the bedding (S) in the Miri quartzite define an

Table 2
Faults along Nala sections, trend dip and dip directions of faults, lithology across the faults, slip in km and sense of slip (viewing north) are depicted. Silt St: Silt Stone; S.St: Sand Stone, RM: Rilu Member and BM: Bomte Member (see Fig. 2).

Fault name/Nala name (if available)	Trend/dip/dip direction	Lithology across/get terminated	Slip in km	Sense of slip (viewing North)
1. F1–F1 (West of Biku Abu Nala)	N38^{0}W/84^0- NE	(1) Silt-Stone, Carb-shale and S.St of Bomte Member terminated against Dafla S. St in the SE and Pink Miri Quartzite in the NW(2) SiltSt of BM terminating against MQ and S.St. of BM	(1)0.02 km against Miri Q and (2)0.125 km against Dafla S. St	Dextral
2. F2–F2 along Biku Abu Nala	N15^{0}E/82^0-WNW	(1)Silt St. of BM against Miri Quartzite and (2) S. St of the BM against Dafla S.St	(1)0.018 km against Miri Q and (2)0.025 km against Dafla S.St.	Sinistral
3. F3–F3 (East of Biku Abu Nala)	N20^{0}E/86^0-WNW	(1)Silt St of the BM against pink Miri Quartzite and (2)Shale, S.St of BM against Dafla S.St.	(1)0.25 km against MiriQ and (2) 0.023 km against Dafla S.St	Sinistral
4. F4–F4 (East of Biku Abu Nala)	N17^{0}E/88^0-WNW	(1) S.St of the BM against Miri quartzite and (2) Silt Stone and sandstone of the Bomte Member against Dafla S.St	(1)0.25 km against MiriQ and (2)0.13 km against Dafla S.St	Sinistral
5. F5–F5 (East of Biku Abu Nala)	N11^{0}E/87^0-WNW	(1) Silt.St. of the BM against white Miri Quartzite and (2) Silt Stone S.St and Carb shale of the Bomte member against Dafla S.St.	(1)0.17 km against Miri Q and (2)0.25 km against Dafla S.St	Sinistral
6. F6–F6 (along Sigen River)	N29^{0}E/86^0-NW	(1)Abrupt termination of the Silt St of the BM against Miri Quartzite (2) Carb shale of Bomte member terminated against Dafla S. St.	(1)0.53 km against Miri Q and (2)0.019 km against Dafla S.St	Sinistral
7. F7–F7 (along Takso Nala)	N31^{0}W/86^0-ENE	(1)Khaki shale, Carb shale and s.st of the Rilu member against Pink and white Miri Quartzite and (2) S.St, Carb shale of Bomte member against Dafla S,St	(1)0.925 km against Miri Q and (2) 0.535 km against Dafla S.St	Dextral
8. F8–F8 (along Garu nala)	N40^{0}W/88^0-NE	(1) Carb shale, coal, Khaki shale of Rilu member against White Miri Quartzite and (2) carb shale, S. St of Bomte member against micaceous Dafla S.St	(1)0.425 km against MiriQ and (2) 0.155 km against Dafla S. St.	Dextral
9. F9–F9 (east of Garu nala)	N35^{0}W/89^0-NE	(1) S.St, Carbonaceous shale of Rilu Member terminating against Miri quartzite (2) S.St of Bomte member terminating Carb shale of Bomte M and against Dafla S.St	(1)0.41 km against Miri Q and (2) 0.24 km against Dafla S.St	Dextral
10.F10–F10 (along Kulu nala)	N39^{0}W/87^0-NE	(1)Diamictite terminating against the MQ (2) Khaki shale and Carb shale terminating against the Dafla sandstone	(1)0.15 km against Miri Q and (2)0.16 km against Dafla S.St	Dextral
11.F11–F11 (East of Kulu nala)	N43^{0}W/88^0-NE	(1)Not extended up to the Miri Thrust (2) termination of carb shale against diamictite (3) Sandstone, catb shale and khaki shale terminating against the Dafla S.St	(2)0.025 km against Rilu Member and (3) 0.29 km against Dafla S.St	Dextral
12.F12–F12 (east of Kulu nala)	N46^{0}W/86^0-NE	(1)Not extended up to the Miri Thrust (2) Orthoquartzite and diamictite terminating against Khaki shale (3) Minor termination of carb shale against Dafla S,St	(2) 0.018 km against Rilu Member and (3) 0.021 km against Dafla S.St	Dextral
13.F13–F13 (along Siki nala)	N54^{0}W/88^0-NE	(1)Diamictite terminates against MiriQ (2) Termination of diamictite against orthoquartzite (3) Minor termination of Carb shale and khaki shale against Dafla S.St	(1) 0.022 km against Miri Q and (3)0.024 km against Dafla S.St	Dextral
14.F14–F14 (along Daring river)	N15^{0}E/85^{0}WNW	(1)Not extended up to Miri Thrust (2) orthoquartzite terminates against the silt stone (3) carb shale and S.St of Bomte M. Terminates against Dafla S.St	(2) 0.017 km against Rilu Member and (3) 0.24 km against Dafla S.St	Sinistral

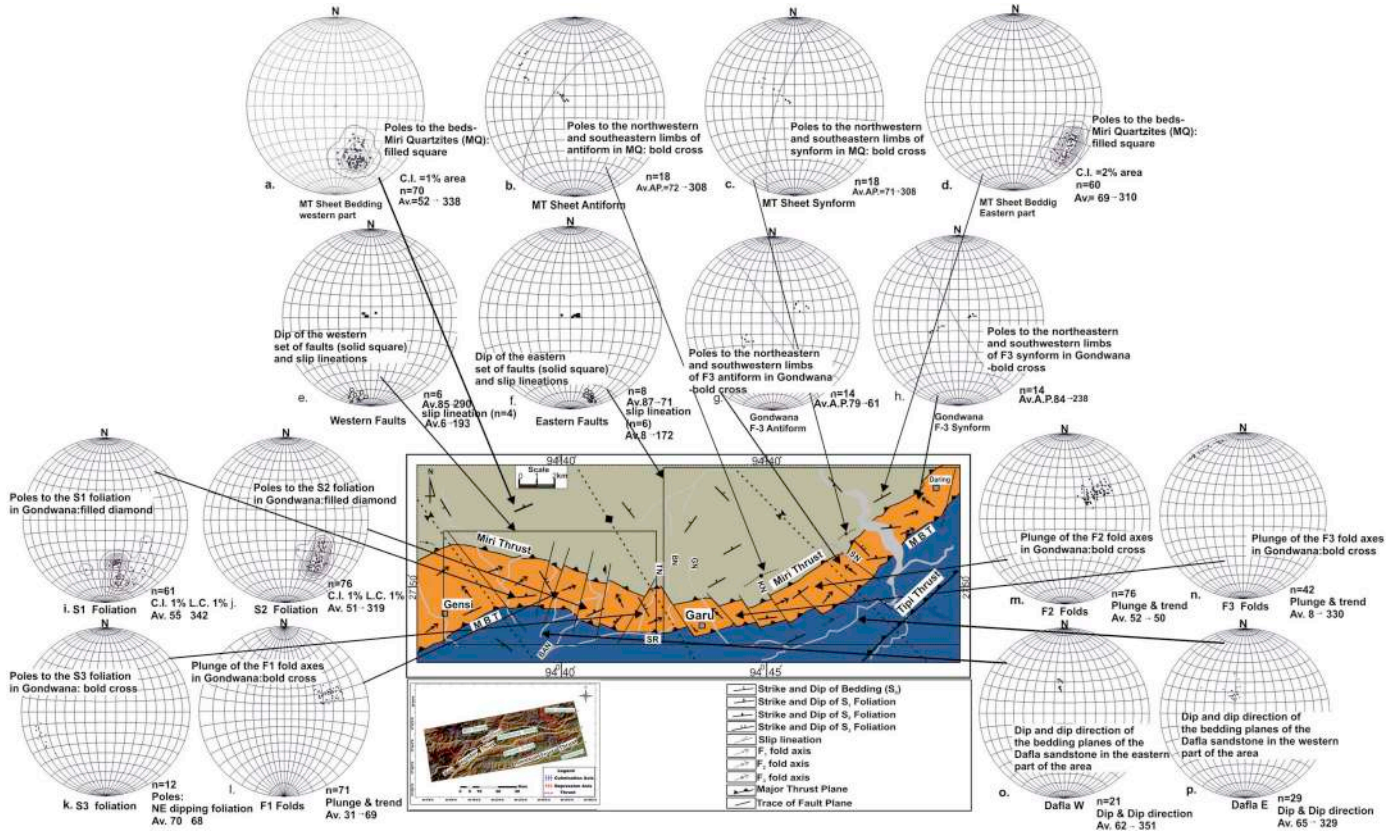

Fig. 3. Structural map of Daring-Garu-Gensi area (prepared by these authors). Equal area and lower –hemisphere projections of poles to the bedding, foliations, fold axis and slip lineations data from the area: (**a**) Poles to the beds of the Miri Quartzites; dominant dip being towards NW from the upstream sections of Biku Abu nala. (**b**) and (**c**). Poles to the limbs define antiform and synform in Miri quartzites from the upstream areas of Kulu nala and Siki nalas.(**d**) Poles to the beds of Miri quartzites; dominant dip being towards NW from the Siki nala and Igo River.(**e**) Average dip of the western set of faults 85° towards 290°; Striae in the carbonaceous shale plunge at low angle (6°) towards SSW direction. (**f**) Eastern set of faults with average plunge of the striae in the grey shale plunge at low angle (8°) towards SSE direction. (**g**) Outcrop scale antiform (F3) in Gondwana sequence measured along Biku Abu, Sigen, Takso, Kulu, Siki nalas; average axial plane dip 79° towards 61°. (**h**) Outcrop scale synform in Gondwana sequence along the nala sections as mentioned in **(g)** average axial plane dip 84° towards 238°.(**i**) Poles to tectonic foliation (S1) in Gondwana sequence from the upstream of Kulu nala(**j**) tectonic foliation (S2) in Gondwana sequence from the Garu nala; average being 51° towards 319°. (**k**) Poles to the S3 foliation in Gondwana sequence average along Sikinala section. **(l)** F1 fold axis lineation in Gondwana sequence from the Takso. nala sections. (**m**) F2 fold axis lineation data from the Gondwana sequences along Kulu nala sections (**n**) Fold axis lineation data for F3 folds in Gondwana sequence along Bomte nala (**o**) and (**p**) the Dafla sequence in the western and eastern part of the area dip at moderate angles (62-64°) to the NW directions. The best fit great circle inferred from the girdle indicates fold axis deduced from the poles to the bedding. C.I.: Contour Interval.

acute angle (~30°). Fig. 6a further shows the thrust contact between the Gondwana and the Miri quartzites, along the Bomte nala section. The slivers of quartzite within carbonaceous and grey-shale of Gondwana exist at several nala sections. These zones of imbrications shows massive asymmetric quartzite pods with top-to-SE and top-to-SW shear within or wrapped by 40–50 cm thick grey to black shale domains. The quartzite pods assume sigmoid geometry (similar to sigmoid mineral fish: Mukherjee, 2011) and connote the shear sense (Fig. 6b and c). In the Sigen and Siki nala sections, in the deformed grey shale and carbonaceous shales, striae plunging at very low angles towards SW and SE are recorded (Fig. 3b,c,e,f).

In the western part of the area (Biku Abu nala section), the grey-shale sandstone units are tightly folded to Class- II geometry and their curved axial planes are ~ 30–40 cm long. The axial plane trends ~ ENE and dip ~ 70° towards WSW. The tightness of the fold decreases remarkably: the interlimb angle elevates from 34 to 56° towards SE over ~1.5 m length possibly indicates deformation partitioning. The tight fold (Fig. 6d) verges NNE, therefore it can be called a back-structure in the Himalayan tectonic context, and is a shear-induced fold. The mesoscale ENE-WSW antiforms and synforms in the Miri group of rocks are related to the D1 and the D2 compressional phases (as per our interpretation and categorization) of deformation with compression being N–S directed. However, the digitally processed image (Fig. 3 inset) indicates regional warps with NW-SE axis of culminations and depressions. This phase of deformation is correlated with compression from east due to the significant impact of the Burmese/Myanmar plate (Singh, 1993).

6. Deformation of the Lower Gondwana (LG) sequences

The mesoscopic structures in the LG sequence in the north of MBT include planar elements such as slaty cleavages, different generations of folds, faults and shear zones. Four deformation phases (D_1–D_4) are identified in the Lower Gondwana sequence in the present study. D_1 and D_2 deformation correlate with the Miocene Himalayan orogeny where strong N–S horizontal compressions folded and thrust the lithounits. Two phases of folding (Singh et al., 1983) and associated structures are correlated with the D_1 and the D_2 phases. The S_1-plane is the most pervasive meso-structure. The S_1 slaty cleavage is defined by parallel alignment of flaky minerals such as muscovite, biotite and chlorite mostly in the Lower Gondwana carbonaceous shales and siltstones. S_1 parallels S_0, the later being the compositional layering within the sandstones. S_1 Strikes ENE with moderate to high dip (40-70°) towards NNW (Figs. 3i and 7a) and is axial planar to the tight isoclinal F_1 folds. The second generation crenulation cleavage S_2 makes 25-30° angle with the S_1 in the silty shale unit of the Lower Gondwana Group

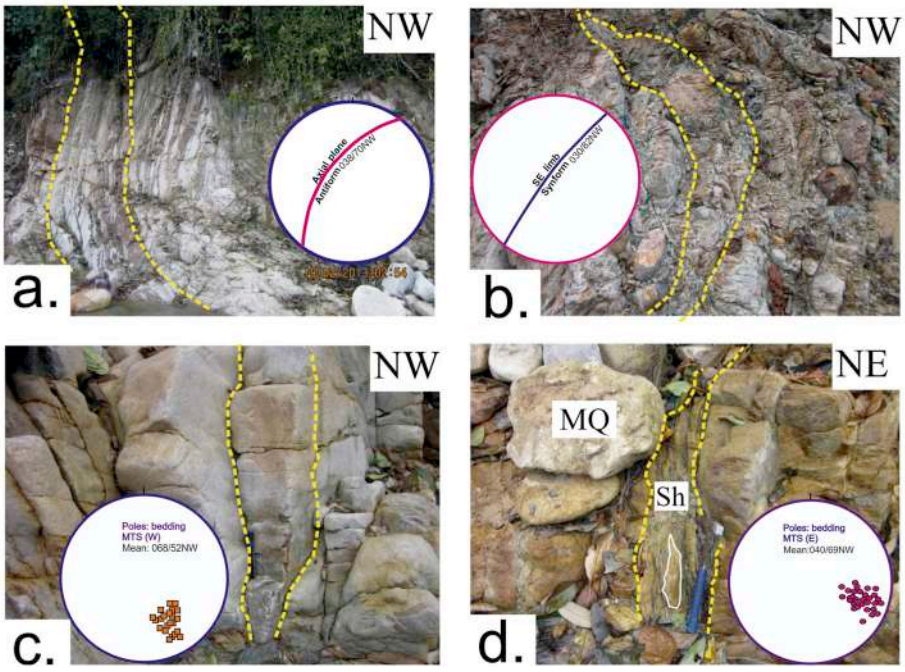

Fig. 4. (a) and **(b).** Two limbs of a synform in Miri Quartzite in Siki nala. The axial plane of antiform and synform dip 72° and 71° towards NW. The steep NW limb of synform shows limb-parallel brittle shear leading to brecciation. Stereoplots: attitude of the axial planes of the antiform and synform**c**. Subvertical beds of Miri quartzites in Siki nala. Poles of the bedding MTS (W) in the stereonet. **d**. Miri quartzites and shale beds in Takso nala. Poles of the bedding MTS (E) in the stereonet with mean.

(Figs. 3j and 7a). These S_2-planes are axial planar to the open asymmetric F_2 folds in the phyllitic siltstone and sandstone units of the Lower Gondwana (Fig. 7b–d). S_2 trends ~ NE with moderate to steep dip (35-65°) towards NW (Fig. 3j). S_3 fracture cleavages associated with the silty shale unit of the Lower Gondwana Group trends WNW and dips at high angle (~70°) towards NE (Figs. 3k and 7d). S_3 makes acute angle to perpendicular relationship with S_1 and S_2 and is not as pervasive as the S_1 and the S_2. Therefore, the first generations of mesoscopic axial planar slaty cleavages (S_1) and the second generation crenulation cleavage (S_2) are significant mesocopic structures within the Gondwana thrust sheet.

Two generations of folds (F_1 and F_2) are frequent in the carbonaceous shales, silty shales, phylitic siltstones and sandstones of the Lower Gondwana Group and are testimonies of the D_1 and D_2 compressional phases of deformation. The F_1 folds are well documented in the phyllitic siltstone, silty shale and sandstone bands of the Lower Gondwana rocks as per the present study. The F_1 folds affect the bedding (S_0) producing tight-isoclinal to reclined folds. These F_1 folds plunge moderately (20-40°) towards ENE (Figs. 3l and 7b-d). Axial planes of the F_1 folds dip moderate to steeply (40-70°) towards NNW. The F_1 folds are refolded by open asymmetric F_2 folds, which plunge 35-65° towards NE (Figs. 3m and 7b-d). F_2 folds are also represented by fine puckers within the phyllitic siltstone unit, where these folds are mostly gently dipping with isoclinal geometries with varying wavelength to amplitude ratios (Fig. 7c and d). At places, the F_2 fold axis is gently curved (Fig. 7b and c) indicating that it refolded to open F_3 folds. F_2 folds have thicker hinge zones and thinner limbs and based on our measurements of orthogonal and axial plane parallel thickness on the limbs these folds are identified as the Class 1C and Class 2 folds as per Ramsay (1967). F_1 and F_2 hinges are near-parallel and represent a type-3 refolding (Fig. 7d). F_2

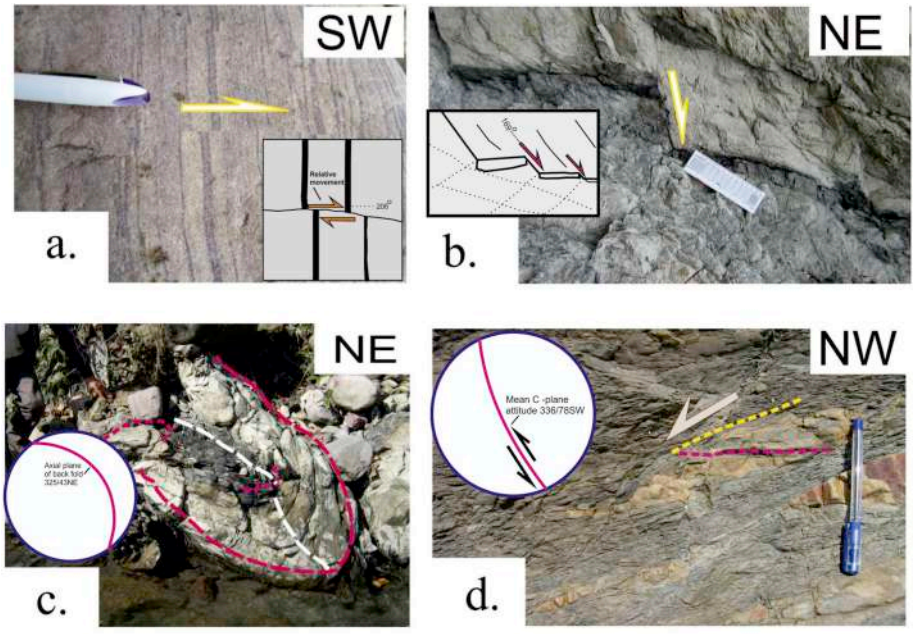

Fig. 5. Eastern and western fault zone: (**a**) SW directed fault in the Miri quartzite in plan. View direction is towards southeast. Sense and direction of the relative movement in the box. (**b**) SSE-directed fault in Gondwana sandstone –shale sequence viewed looking northerly. Sense and direction of the relative movement in the box. (**c**) Fault zone in the Gondwana rocks. The observed portion of the fault zone is a tightly recline folded. The axial plane of the fold trends NW and dips steeply towards NE. Curved fold hinge line marked with yellow and white lines. Stereoplot: attitude of the axial plane of the back fold. (**d**) Slivers of Miri quartzite within Gondwana shale bed. The trace of the bedding in MQ and the shear foliation (arrow) are shown as red and yellow dashed lines, respectively. Stereoplot: mean C-Plane attitude. (For interpretation of the references to colour in this figure legend, the reader is referred to the Web version of this article.)

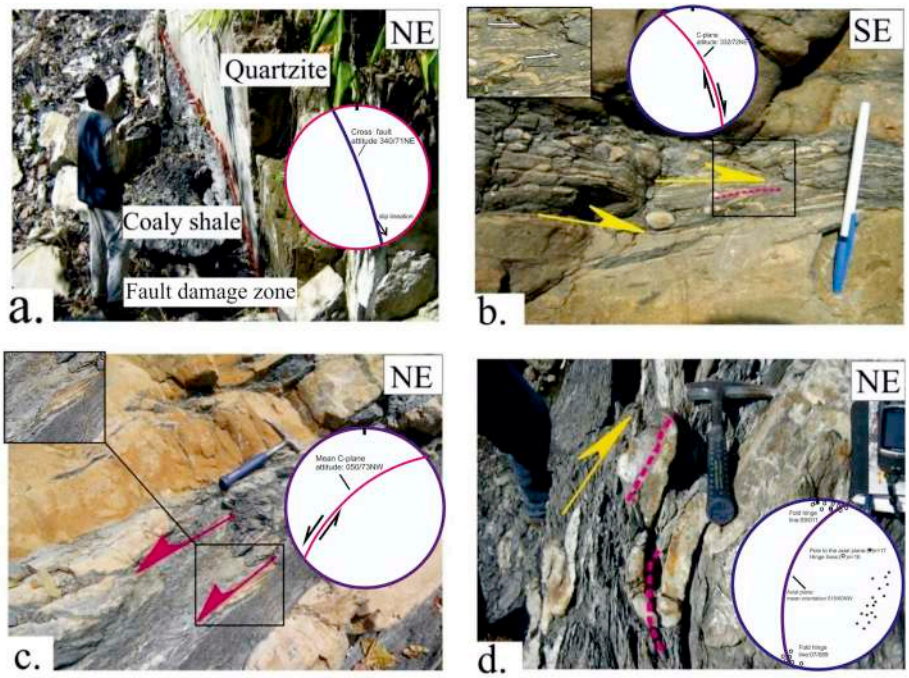

Fig. 6. (a) Faulted contact between the Lower Gondwana and the Miri Group at Bomte and the exposed fault damage zone, Stereoplot: attitude of the cross fault and slip lineation. **(b)**. Slivers of Miri quartzite within the grey shale of Gondwana (Siki nala). Quartzites top-to-SE sheared (inset). Near horizontal striae in the grey shale indicate a dextral sense. Stereoplot: attitude of the C-Plane **(c)** In the Sigen nala section, sheared pink quartzites within carbonaceous shale of Gondwana. The quartzites show top to the SW (sinistral) shear sense (as seen in plan) reddish orthoquartzite and grey shale exhibit competency contrast while responding to high shear stress. The horizontal movement is indicated by striae in the carbonaceous shale plunging at very low angle to SW. Stereoplot: mean attitude of the C-Plane. **(d)** Grey and reddish sandstone-silt stone domain tightly folded in grey shale. Stereoplot: mean orientation of the axial plane and hinge lines. (For interpretation of the references to colour in this figure legend, the reader is referred to the Web version of this article.)

folds can be correlated to ENE trending isoclinal F_4 folds in Lower Gondwana reported by Kumar (1997).

F_3 folds created due to the refolding of the F_2 folds are NW-SE folds and plunge at ~ 7-10° to NW (Fig. 3n). These folds are also manifested commonly by gently NW plunging (~15°) disharmonic folds and kink bands near the Garu nala. F_3 may be correlated to a D_3 compression along E-W due to the Indo-Burmese collision during Late Oligocene or Early Miocene (Goswami et al., 2017). The Siang antiform (~50 km east of the study area) with curved MBT as roof thrust and Palaeocene-Eocene sequence at its core developed presumably during this deformation (Kesari, 2010). Note that the trend of the F_3 axis and the axis of the regional warps on a digitally processed image for lineaments in the study area (Fig. 3 Inset), are observed to be roughly parallel (Fig. 3g and h). Further, the NNW plunging F_3 folds can also correlate with the ~N–S folds of D_3 phase of deformation in the low-grade meta-sedimentary sequences of the lower Siyom valley (Singh, 1993). D_3 deformation may be correlated to D_5 deformation in the (Kumar, 1997) which produced NW trending folds in the Lower Gondwana sequence.

The combined compression due to the impact of the Burmese plate and the Asian plate may be resolved into a resultant compression from N/NE direction probably during the Late Pleistocene. We correlate this D_4 deformation with a brittle phase, which helped the development of transverse faults and eventual offsets in the MT and MBT. It is estimated that the India-Asia collision accommodated a shortening of ~239 km across the NW-SE trending thrusts of Mishmi block with a shortening strain of 83.28% (Ningthoujam et al., 2015). Considering this, the compression direction has to be along NE-SW direction orthogonal to NW-SE trending Mishmi, Lalpani, Tidding and Lohit Thrusts in the Mishmi block. Further NNE-SSW trending dextral oblique-slip Tuting–Igo fault on the left limb of the NNW plunging Siang window (Ding et al., 2001) indicates that the direction of the resolved compressional stress for combined India-Asia and India-Burma collision has to be

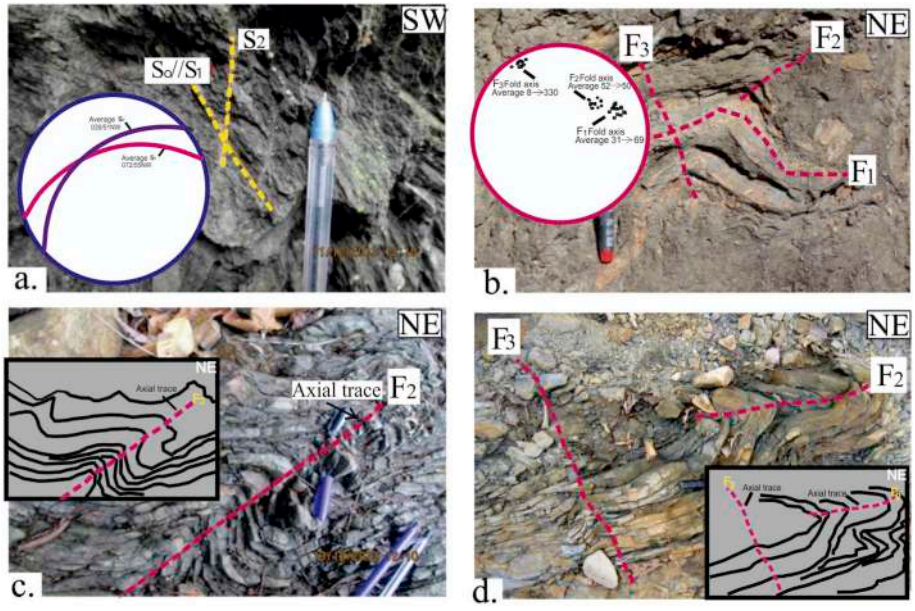

Fig. 7. Lower Gondwana shale, sandstone and siltstone showing different generations of folds and foliations. Stereoplot: average orientation of S_0 and S_1 **(a)** $S_0//S_1$ having acute angle relationship with S_2 in Lower Gondwana shale, (**b**) Sub parallel axes of F1 and F2. Stereoplot: average orientations of F1, F2 and F3 fold axes **(c)** Second generation S_2 cleavages axial planar to the open fold (F_2) in the phyllitic siltstone and sandstone units. Line drawing in the box: F2 axial trace (**d**) S_3 fracture cleavages associated with the silty shale unit of the Lower Gondwana Group trends WNW to E. S_2trends cleavage trends NE-SW. Line drawing in the box: F2 and F3 axial traces.

along NE-SW direction.

Three generations of folds (F_1–F_3) in the Miri Group of rocks was reported by Singh et al., (1983). However, there is a mismatch in regard to trend of the F_1, F_2 and F_3 folds reported by Singh et al. (1983). The south verging antiform and synforms in the Miri Group of rocks resulted due to strong horizontal NS compression. The F_3 folds both in the Gondwana and the Miri rocks are NW-SE trending warps due to the impact of Burmese plate from eastern direction. We interpret that F_1 –F_3 folds represent three phases of deformation (D_1-D_3). The subsequent brittle phase (D_4) also affected both Miris and Gondwanas and responsible for the formation of the transverse fault zones. The kinematic detail of transition from ductile to brittle ductile to completely brittle deformation regime would require more focused study.

7. Transverse faults across the MBT

In the regional scale, MBT forms a fault-bend antiform trending NW (Basa et al., 2019). Earlier studies in the present area have depicted the MBT to be a sharp contact between the hangingwall: the Gondwana and Miri sequences, and the footwall: the Lower Siwalik Dafla sandstones (Singh and Chowdhury, 1990; Jodha, 1991; Singh, 1993; Kumar, 1997; Yin, 2006). However, we note that faulting and shear have obscured any simple contact relation. The offsets in the MBT transcend the Gondawana and the Miri sequences and different kinematic indicators indicate both dextral and sinistral shears, the dextral sense being dominant (Figs. 2 and 3).

The southern extension of the Lower Gondwana rocks ends abruptly against the irregular and high altitude hills constituted by the Dafla Formation of the Siwalik Group near the location Garu. The ENE trending contact between the Siwalik and the Gondwana, the MBT, with a high northerly dip (~65°) is traced from Daring in the east (29 km from Garu) to Gensi in the west (32 km from Garu). The contact was observed along the nala/foot track sections only (Fig. 8). Due to the thick vegetation and inaccessibility, the contact could be tracked further neither in field nor in the remote sensing image. The nine contact zones are offsets in MBT about ~ 5–30 m thick and are marked by extensively crushed and pulverized rocks. Along-strike variation in the thickness of these zones (~ 30–50 m) is marked for ~ 35 km (Figs. 2 and 3). Two contact zones between the Gondwana and the Dafla sequences are observed in the Sigi-Takso nala sections. The open to tightly folded NE-SW trending sandstone-shale sequence of the Dafla Formation show top-to–SE shear in terms of sigmoids in the sandstone. The shale bed is almost pulverized. Sigmoid lenses of sandstones are also observed within the shale beds (Fig. 8a).

The W-dipping Dafla sandstone in the Takso nala shows strike-slip, which is observed both in horizontal and in vertical section (Fig. 8b). The sandstone-shale sequence in Fig. 8a also represents a gouge zone, which can be better observed in the lower right corner of the same photograph. The fault zones in the Dafla sequence observed in other locations demonstrate both top-to-SE and top-to-SW shear, the former sense being dominant. The cross-cut between these shear planes are not found, therefore their relative timing remains indeterminate.

8. Seismicity

The ISC and the USGS earthquake database of 6665 seismic events during 1901–2018 with 4.0–6.6 magnitude with focal depth 4–200 km were used to prepare an epicentral location map (Fig. 9a and b). Epicentres of the magnitude 5.6 to 6.0 in the depth range of 20–30 km in the area of study show nearly a linear NNW trend parallel to the Tuting-Igo Fault indicating seismogenic nature (Fig. 9a and b). During the period, the region experienced ~55% of the earthquakes with 4–4.5 magnitude. The presence of moderate earthquakes ($M \geq 5$) in the region indicates that the strain accumulation has been taking place in different segments. From the analysis of earthquake data during 1901–2018, 1010 events of earthquakes of magnitudes 5.1 to 6.0 occurred in the area with 20–60 km focal depth (Fig. 9a and b).

Following the 1950 great Assam earthquake ($M = 8.6$; epicentre near Rima, Tibet) another earthquake of $M = 7.7$ took place ($M = 7.7$; epicentre at Manipur–Burma border) in 1954. During the period (1943–2016) the region also experienced major earthquakes due to the dextral-slip along the orogen-transverse Kopili lineament (1943, M7.5 and 2016, M6.7; Srivastava et al., 2013). This NW-SE trending fault extends up to Bhutan (Kayal et al., 2010). Further, the NW-SE trending Bomdila Fault is considered to be responsible for the straightening of the courses of Dhansiri, Brahmaputra, Burai and Bargang rivers to the NW. A numbers of large magnitude ($M > 5.5$) seismicity close to the Bomdila Fault are recorded (Sarma and Sharma, 2018).

The tectonic landforms in the present study area not only affected by movements along MBT and HFT, but by later formed transverse faults (Bhakuni et al., 2017). Along the Dikrong river valley, both upper and Middle Siwalik sequences are affected by the NW-SE trending Banderdewa Fault and the entire zone shows concentration of the epicentral locations of large number of low magnitude ($M \leq 4$) earthquakes (Devi et al., 2010). In Fig. 9a and b large magnitude ($M \geq 6$) earthquakes recorded within a depth range 30–80 km, both north and south of MBT, indicates the seismic vulnerability in the present study area. Further geophysical data may help us to constrain a better model in future.

There are records of earthquakes (with foci located in the Himalayan arc and its fore deep) associated with transverse faults in the region. With the northward advancement of the Indian plate, these faults become active seismic blocks which produce conjugate shear fault pattern (Dasgupta et al., 2013). The present study focuses on the analysis of the outcrop-scale geometry of the conjugate shear faults and their connectivity with the seismogenic faults in the area. The continuity of the lateral slip along these faults, tens of km south of MBT in the highly populated foredeep (Brahmaputra valley) is highlighted. Thus the data pertaining to the structural analyses of the present study may be invaluable in the formulation of strategies to cope with seismic vulnerability of the region.

9. Tectonic synthesis

During early Middle Miocene (10–12 Ma), the Gondwana got

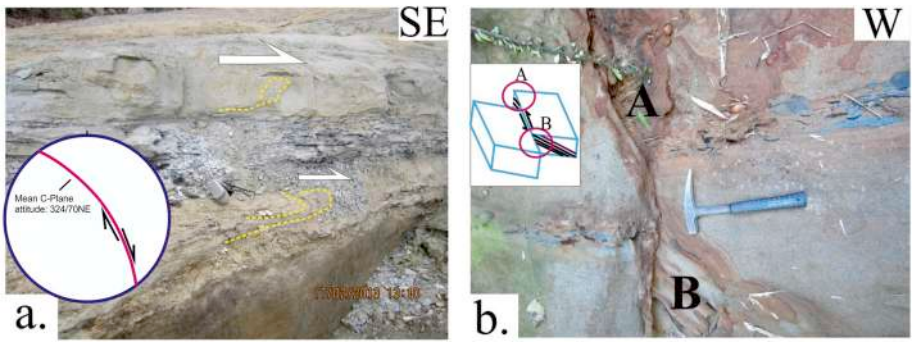

Fig. 8. (a) The thrust contact (MBT) between the Gondwana and the Dafla rocks. The MBT trends NE. The Gondwana sandstone pinches out against the MBT. Stereoplot: attitude of the mean C-plane. (**b**) Dafla sandstone trends NE. The core part of an open antiform is shown. The antiform verges towards SE. Inset: A & B -the NS and EW section of the sinistrally moving right side block.

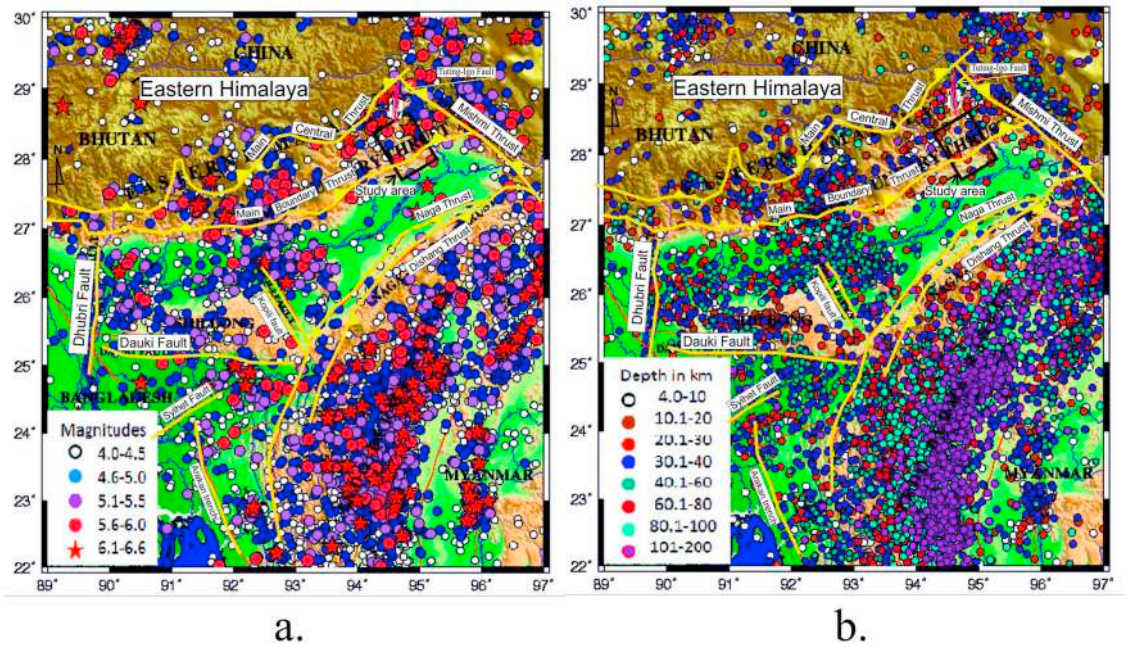

Fig. 9. The epicentral plot (The ISC and USGS database) **(a)** variation in magnitude and **(b)** variation in depth as observed in NE India for a time range of 1901–2018. The present study area is shown within bold rectangle. (c) The epicentral plot (The ISC and USGS database) (a) variation in magnitude (b) variation in depth as observed in NE India for a time range of 1901–2018. The present study area is shown within bold yellow rectangle. (For interpretation of the references to colour in this figure legend, the reader is referred to the Web version of this article.)

uplifted by the MBT (Huyghe et al., 2001; Yin, 2006). Therefore, the structures of the $D_1$and theD_2 deformation phases in the Gondwana sediments in the study area are presumably syn-Himalayan or Neo-Himalayan: ~18 Ma (Mukherjee et al., 2016). Unlike the other Himalayan parts, the impact of the Burmese plate in the present area represents an additional constrain, which is a major factor for the tectonic evolution of the Gondwana rocks (Singh, 1993; Acharyya, 2015). The NW/WNW directed impact of the Burmese plate continued till Late Pleistocene or post-Pleistocene.

The ESE or E-directed compression due to the impact of the Burmese plate responsible for the N/NNW plunging open F_3 folding (the D_3 phase) in the Gondwana rocks as well as the N/NNW trending broad warps in the Miri, the Gondwana and the Siwalik rocks in the area are important. These ~ N–S folds are also comparable with those in Lower Siyom valley (Singh, 1993) and curved traces of major thrust in the northern part of the Siang valley (Ray, 1995; Yin, 2006). *(iii)* Resultant of the combined EW and NS compression producing an effectively NE/NNE-directed compression during Late Pleistocene as the Burmese and the Asian plates collided developing transverse fault zones in the MBT and MT in the area.

The MBT is a splay fault branching out from the Main detachment fault from 15 to 20 km depth (Srivastava and Mitra, 1994 and references therein) probably during the Early Miocene (Srikantia, 1989; Valdiya et al., 1992; Srivastava and Mitra, 1994; Raiverman et al., 1994; Kumar, 1997; Mukul, 2000; De and Kayal, 2003; Shah et al., 2012). Age of the MBT is inferred as 10–12 Ma in eastern Himalaya (Yin, 2006) and the proximity of the MCT and MBT indicates increase in the magnitude of shortening in the eastern Himalaya (Yin, 2006). Based on hypocentral cross-sections for the earthquakes in the AH, it is difficult to record the sub-crustal earthquakes at ~50–80 km depth south to the MBT (Kayal et al., 1993). On the other hand, focal mechanism solutions (Mukhopadhyay, 1984; Dasgupta et al., 1987) suggest deep-seated transverse tectonics.

Further, in Sikkim and AH, the MBT is folded together with the overlying MCT (Acharyya and Ray, 1977; Acharyya, 1980) and this has resulted in duplex development between the MBT above and the MFT below (Yin, 2006). The MBT emplaced and developed a sag basin in front of the thrust where Dafla, Subansiri and Kimins deposited during the Middle-Upper Miocene (Kumar, 1997). Therefore, in one way, the compressive phases that evolved the Sub-Himalayan Siwalik fold and thrust belts (10–12 Ma, Yin, 2006) also affected the Gondwana and the Miri rocks. Moreover, compared to the hard massive Miri quartzites, the carbonaceous shale, phyllite and siltstones of the marine Gondwana successions of the eastern Himalaya are presumably weaker and deformed in response to the Himalayan compression. Gondwanas with incompetent carbonaceous shales, slates and less competent sandstones constituted the folded MBT thrust sheet between the two wedges of Miris and Daflas. Further, we believe that the MBT may be considered as a reactivated fault along the inherited extensional faults within the Gondwanas. Reactivation of the MBT has been inferred from few sections of the Himalaya (e.g., Valdiya, 2001). The folds in the Middle Miocene Dafla sequences in the footwall and Gondwana rocks in the hangingwall differs geometrically (Figs. 6a–d and 7b). On the other hand, folds in the Gondwana and the Miri rocks vary geometrically. The ENE, the NE and the NW trending type-3 superposed folds occur in the Gondwana rocks due to the E-W directed maximum compression probably during Middle to Late Pleistocene.

In the present area the F1folds (Singh, 1993) in the Gondwana sandstone with fold axis plunging at low to moderate angle towards NE must be due to strong (horizontal) ~ N–S compression due to the India-Asia collision. The same compression produced south verging antiforms and synforms (during D_1-D_2 phases) in the more competent Miri quartzites. In the fault zones the axial planes of these mesoscopic folds in the Miri Quartzites dip steeply northerly. Away from the fault zones, the superposed deformation in the Gondwana sequence between the Garu nala and the Siki nala (Fig. 2) shows an E-W compression, which may be due to the tectonic imprint of the Burmese plate. Following this, the compressions from N followed by NE are responsible for development of conjugate faults in the area where dextral displacement becomes more prominent. In the regional scale Tuting-Igo fault is a dextral fault (Fig. 1). In the present work Fault No. 7 shows maximum displacement among the faults (Fault No. 7; Fig. 2) which show dextral sense of displacement.

The three generations of folds, F_1 to F_3, obviously represent ductile

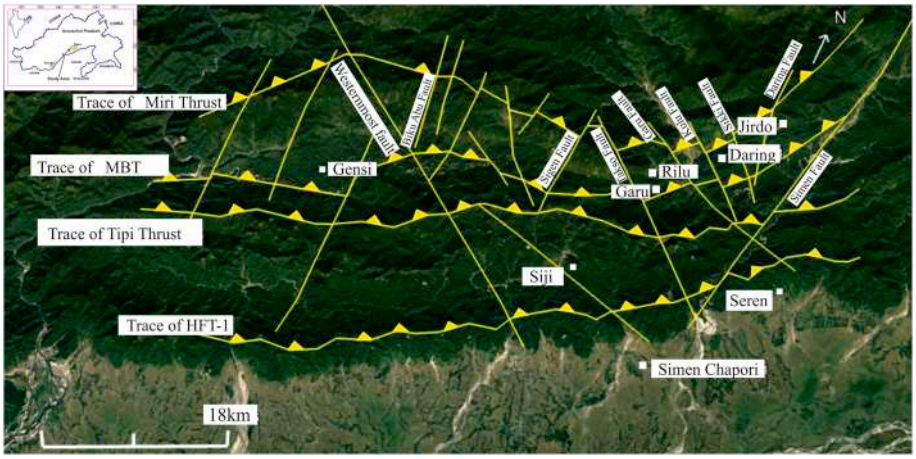

Fig. 10. Google image with traces of major thrusts (MT, MBT and HFT-1). The cross-faults (of Group-I and Group–II– see text for details) are shown.

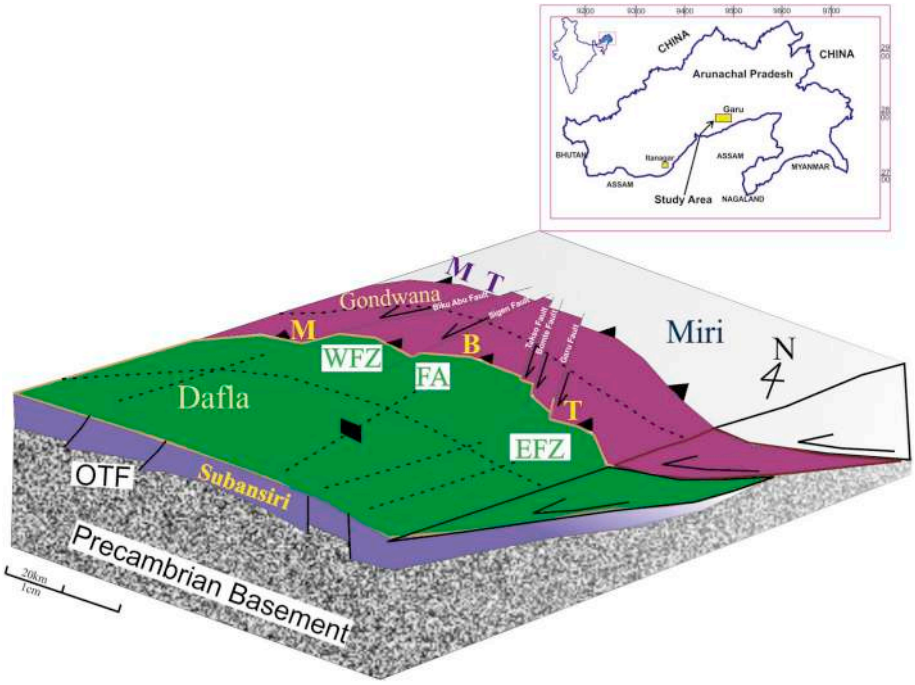

Fig. 11. Cartoon illustrating folded Miri, Gondwana and Dafla thrust sheets and Miri Thrust (MT), Main Boundary Thrust (MBT). Orogen-transverse fractures (OTF) in Precambrian basement and NW-SE trending fold axis (FA) of the open fold and Western and Eastern Fault Zones (WFZ &EFZ) shown.

deformation in the Gondwana sequence. However, the extension in the long limb of the asymmetric F_2 folds and formation of competent layer boudinage represent brittle deformation. We have mapped only the outcrop-scale antiforms and synforms in the Dafla sandstones-shale sequence for ~30 km^2. The D_4 represents a dominant compression from NE/NNE due to the combined N–S impact of Asian and ~ E-W impact of the Burmese plate. This produced two sets of NE-SW and NW-SE trending transverse fault zonesor offsets for a strike length of ~60kmalong the MBT (Figs. 2 and 3). Both the hangingwall and the footwall sequences of the MBT are affected by these transverse faults (Figs. 10 and 11). The Miri- Gondwana thrust contact is obscured by the later transverse fault zones as mapped along Siki, Sigen Takso and Bomte nalas (Figs. 2 and 3). These fault zones are ~50–80 m thick. The slivers of Miri quartzites occur within the Gondwana shales. Numerous fault related folds are observed along the fault zones across Miri-Gondwana sequence. These folds and sigmoid sandstone pods connote ductile shear and has to be associated with the MBT thrust ramp. These structures nucleated plausibly in a strike-slip stress field configuration (Tavani et al., 2015) which we consider here as D4 phase. In the Lower Siwalik Dafla sandstones and shales, these fault zones are manifested as ~30–40 m thick zones of imbrications and slip sense can be observed both in plan and in sections.

An increase in the amount of slip in the eastern fault zones (0.925 km along Takso; 0.425 km along Garu nala) might indicate anincrease in the amount of the angle between the direction of compression from N to NE (during late Pleistocene time) and direction of shear as observed in fault zones from Garu to Daring. The angle between the compression direction and the initial orientation of the fault planes in the present case is more than 30°as observed in regard to stability of the fault pattern during finite strain deformation (Anderson, 1942; Yin and Taylor, 2011 and references therein). However, strike of the eastern fault zones as measured from the field (Garu, Siki, Takso, Kulu Faults) indicate fault plane strike at an angle of ~40° with the compression direction oriented NNE (Fig. 12a–c).

Anderson (1905) proposed the pure shear mechanism for conjugate strike-slip faults. It is proposed that dextral and sinistral strike-slip

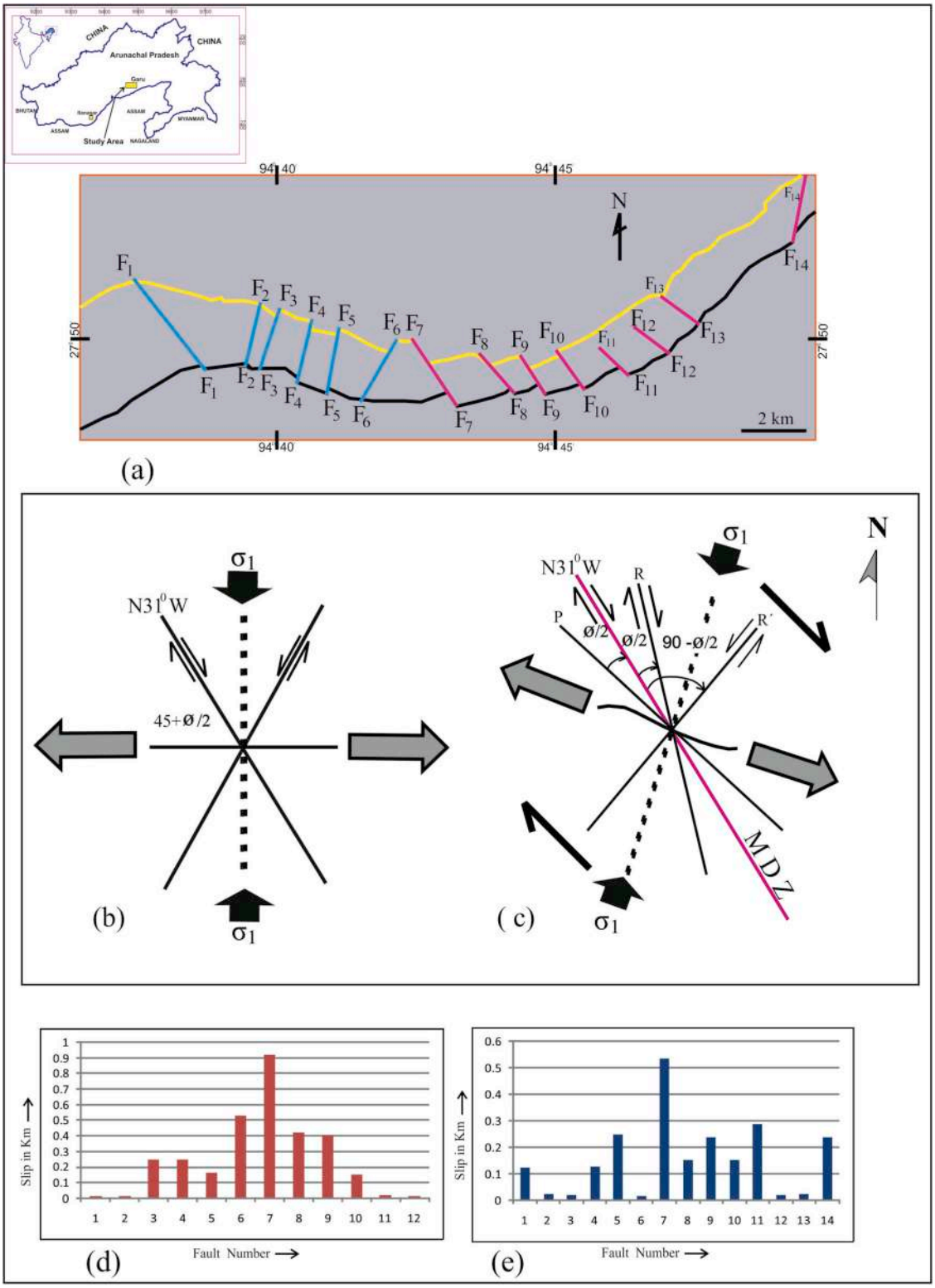

Fig. 12. a. Group-1 faults (red) (F7 to F14) and Group-II faults (blue) (F1 to F6) (see Figs. 2 and 3). b. Coloumb –Anderson model for pure shear (Sylvester, 1988). **c.** Right simple shear (Reidal model). Bold dashed line for extension fractures (or T-fractures); the fold axis is represented by a wavy line; P=P fractures; R and R' for synthetic and antithetic fractures; MDZ: Main Displacement Zone; short solid arrows for compression (σ_1) (Sylvester, 1988). Histogram for fault slip in km for Miri-Gondwana and for **(d)** Gondwana –Lower Siwalik cross faults. **(e)** Fault No. 7 clearly shows maximum displacement. (For interpretation of the references to colour in this figure legend, the reader is referred to the Web version of this article.)

faults form an angle of Ø and – Ø, with the compression direction (Sylvester, 1988). Here Ø is the angle of internal friction (Fig. 12b and c). In this model, the principal stress axis is considered to be parallel to the principal strain axes. Under this condition, conjugate strike-slip faults have to operate simultaneously if they have to accommodate the irrotational bulk strain (Sylvester, 1988). As a result, any space problem created in the process has to be solved by rotation and alternating differential displacement on each of the faults. In the present study, we

are ruling out this possibility as the axis of compression rotated clockwise from being NS to NE-SW direction. Therefore, here the strike-slip faults depict a simple shear model (Fig. 12c). The associated structures are synthetic (NW-SE trending: F7–F13) (Cloos, 1928) and antithetic strike-slip faults (NE-SW trending: F2–F6) (Tchalenco, 1970) or R and R′ Riedel shears. Considering the orientation, F_1 fault can be termed as 'P' strike-slip fault that make an angle of ~20° to the Main Displacement Zone (MDZ). The MDZ is along the Takso nala, which can be designated as 'Y' strike-slip fault in regard to the assembly of structures associated with simple shear model of conjugate strike-slip faults. The fault slip shown with histograms (Fig. 12d and e) for both Miri- Gondwana and Gondwana-Lower Siwalik thrust contact shows Fault −7 to be the MDZ (Fig. 12c).

Geological structures in collisional orogens form by a combination of internal deformation and translation of material points in rocks towards the foreland for an overall mono-vergent wedge such as the Himalaya. For example, drag folds form coevally on a moving thrust sheet (Mukherjee, 2014, 2017). Fault propagation folds in the MBT hanging wall are quite common structures. Orogen-transverse strike-slip faults in the large-scale thrust are usually the youngest structures (Nakata, 1989) though not necessarily neotectonic. During the initiation of the strong horizontal N–S compression during the Early Miocene followed by combined compression along N–S and E-W, rocks folded thrice (F1 to F3). Google Earth image also helped to constrain the traces of major thrusts (MT, MBT and HFT-1) and the cross-faults that have affected the Kimins, the youngest Siwalik rocks in the area, developing sinuous mountain fronts for ~ 70 km (Fig. 10).

Two sets of conjugate faults and offsets in the MT and MBT are further depicted in the cartoon (Fig. 11; eastern sets at: Siki, Garu, Bomte, Takso and western sets at: Sigen and Biku Abu, Fig. 2) [Local faults along the nalas cannot be named as these nalas are unnamed in 1:50,000 topo-sheet]. Transverse faults along MBT are documented based on the field studies. The portrayal of the transverse faults in Figs. 10 and 11 are based on our field studies and transverse faults mapped in the mountain front south of the present area (Bhakuni et al., 2017) and hypocentral cross-sections indicating deep seated seismogenic strike-slip faults in the area (Kayal et al, 1993; 2001). Two shear components associated with compression from NE in the D_4 deformation are depicted (Fig. 12c). Based on NW-SE trending open warps in the Miri, the Gondwana and the Dafla sequences (DEM Image of the area: Fig. 3), the conjugate sets of faults offsetting the MT and the MBT are considered to be culmination phase of deformation in the area. These transverse faults may also be connected to deep-seated seismogenic strike-slip faults (Bhakuni et al., 2017).

10. Hydrocarbon prospectivity

The Upper Assam petroliferous basin is bounded in three sides by Himalaya, the Mishmi block and Indo-Burmese collsional orogen. The tectonic set up of the basin changed temporally due to the collisions and accordingly the depositional environment was also affected (Mandal and Dasgupta, 2013, Fig. 1). In the basin, the Brahmaputra arch is dissected by a number of NE-SW and ENE-WSW trending extensional faults that parallel the regional Naga Thrust (Sahoo and Gogoi, 2011a,b). The details of these faults-whether sealing or leaking is not known. The foreland shelf zones of upper Assam exhibit two prominent sets of extension faults trending NNE-SSW and ENE-WSW. These extension faults were formed in the basement craton and most of the seismic and lithosections in the upper Assam oil field areas have shown that the overlying cover sediments of Barail, Tipam and Girujan sequences are also affected by these faults (Handique and Borgohain, 1984). It is important to note that these extension faults are parallel to the Naga Thrust and offset of these extension faults have taken place by large scale strike slip faults in the basin (Rao, 1983; M Sahoo and Gogoi, 2011a,b).

A pronounced foredeep in front of the Mishmi Thrust and fractures sympathetic to the NW trending Mishmi Thrust in the Brahmaputra valley are well observed (Dasgupta and Biswas, 2000, Fig. 19). On this backdrop, the continuation of the orogen-transverse faults in the AH across the Brahmaputra Arch cannot be ruled out. An investigation in this regard based on more fieldwork and detail study of the remote sensing images can help to understand the migration pathways of hydrocarbon to the north Brahmaputra foredeep. See Appendix for some detail on hydrocarbon occurrence near the study area.

The slip variation along E-W for the faults documented is difficult to measure and elaborate further. The structure contour maps indicate that the downthrow of the extension faults are in the SE direction. Further the throw decreases from 100 m in the NE to 20 m in the SW direction. The major strike slip faults show offset of the strike to the SE direction (Murty, 1983; Pratap et al., 1997; Borgohain and Singh, 1999). In the block faulted foreland shelf areas the faults have acted as conduits for the migration of the hydrocarbons (M. Sahoo and Gogoi, 2011a,b).

11. Conclusions

1. On the basis of the outcrop mapping and study of remote sensing images in the area along the Main Boundary Thrust around the Garu-Gensi area, two conjugate sets of fault zones are demarcated making an angle of ~ 60° showing dextral and sinsitral (brittle–ductile) slip and distributed along a stretch of ~ 70 km. The Miri, the Gondwana and the Lower Siwalik Dafla sequences are affected by this faulting.

2. The north-south compression during Middle Miocene thrust the Gondwana rocks over the Siwalik rocks along the MBT. This compression imprinted deformation in the Gondwana rocks during the D_1 and the D_2-phases. The next D_3-phase in the Gondwana rocks indicates an E-W compression that produced open NS or NNW-SSE folding. This is comparable with the NS folding in the low-grade metasedimentary sequences in the eastern part of the area in the Siyom valley. The open F_3 folds in the Gondawan rocks plunge at low-angle towards NNW. The NNW plunging Siang Antiform, the NS folding in the Lesser Himlayan sequence in the Siyom valley (west of the Siang antiform) and the NW trending F_3 folds in the Gondwana and Miri rocks in the present area, all point to thecompression from the easterly direction due to the Indo-Burmese collision.

3. A late phase of combined compression due to the collsion of the Asian plate (NS) and the Burmese plate (EW) probably during Late Pleistocene produced a resultant compression that acted along NE. This compression developed two sets of conjugate orogen-transverse sinistral and dextral faults zones in the NNW-SSE open folded Gondwana, Miri and the Dafla sequences. This phase of deformation is constraied as the D_4 phase in the present study, which is a new finding.

4. Slip variations along the fault zones are noted along E-W of the study area. The central portion of the fault zones shows maximum slip, which is as expected for a natural faut zone. Dominanlydextral slip occurs mainly at Garu, Siki, Takso and Bomte nala sections. The dextral Reidal shear led to maximum displacement along the NE trending fault-7. Due to the rotation of the compression direction from NS to NE (involving both India-Asia and Indo–Burmese collsion), the synthetic strike slip faults are produced.

5. The reccord of the earthquake events with M ≥ 6 during 1901–2018in the study area suggest a seismogenic orogen-transverse fault within 30–80 km depth across the MBT. This may require further geophysical data for confirming the seismic vulnerability of the region.

6. A thorough study of the southerly continuation of the orogen-transverse faults will help us to constarin the hydrocarbon migration pathways across the Brahmaputra archin the North Assam Shelf.

Credit author statement

SM was involved significantly in revisio9n of the ms and ms writing.

All the other authors produced field data and wrote preliminary ms.

Declaration of competing interest

No conflict of interest with anyone.

Acknowledgements

BNM and BRS are grateful to the Addl. Director General & HOD, NER, Geological Survey of India, Shillong for providing fieldwork facilities. The authors are also thankful to Sh. Amit Kumar, Geologist, GSI, Itanagar for assistance during the fieldwork. TKG and RKS acknowledge the financial assistance received from the UGC-SAP-DRS-II Program in the Department of Applied Geology, Dibrugarh University to carry out the fieldwork. SM thanks CPDA financial support from IIT Bombay. We thank M. Chetia (Dibrugarh University) and Dripta Dutta (IIT Bombay) for assistance. The two anonymous reviewers and the Handling Editor Prof. Adam Bumby are thanked for providing helpful comments.

Appendix

A. Oil wells (Dasgupta and Biswas, 2000).

Drilling operations are completed in the Jonai (~ 50 km from Garu) and Bihpuria (~120 km from Garu) oil wells in the northern part of Brahmaputra, where Barail (Oligocene) and Tipam (Middle Miocene) sequences have been encountered. But the proper correlation with the similar horizons in the southern Brahmaputra basin is yet to be established.

B. Coal deposits (Sarmah, 2013).

In the Makum Coal fields of Margherita coal depsosits are located in the Barail Group of rocks (Oligocene age). The rock types are sandstones, shale and coals. There are five coal fields within the Makum Coal fileds. These are Namdang (~ 130 km from Garu), Boragolai (~ 120 km from Garu), Tipong (~ 132 km from Garu), Ledu (~ 125 km from Garu) and Tirap (~ 136 km from Garu). The lower part of the deposits belongs to argillaceous facies and upper part belongs to arenaceous facies. The colas are of Oligocene age and the grade is Bituminous A, B and C (with high moisture, low ash, medium to high volatile, sulphur and vitrinite rich). These coal deposits stratigraphically belong to Tikak Parbat Formation of the Barail Group of rocks.

Appendix A. Supplementary data

Supplementary data to this article can be found online at https://doi.org/10.1016/j.marpetgeo.2020.104242.

References

Acharyya, S.K., 1980. Structural framework and tectonic evolution of the Eastern Himalaya. Himal. Geol. 10, 412e439.
Acharyya, S.K., 2015. Indo-Burma Range: a belt of accreted microcontinents, ophiolites and Mesozoic–Paleogene flyschoid sediments. Int. J. Earth Sci. 104, 1235–1251.
Acharyya, S.K., Ray, K.K., 1977. Geology of the Darjeeling-Sikkim Himalaya. Guide to Execution No. 4. Fourth Intemational Gondwana Symposium. Geo1. Surv. India, Calcutta, pp. 25p.
Acharyya, S.K., Ghosh, S.C., Ghosh, R.N., Shah, S.C., 1975. The Continental Gondwana Group and associated marine sequence of Arunachal Pradesh. (NEFA) Eastern Himalaya. J. Him. Geol. 5, 60–82.
Adlakha, V., Patel, R.C., Kumar, A., Lal, N., 2019. Tectonic control over exhumation in the Arunachal Himalaya: new constraints from apatite fission track analysis. In: In: Sharma, R., Villa, I., Kumar, S. (Eds.), Crustal Architecture and Evolution of the Himalaya-Karakoram-Tibet Orogen ume 481. Geological Society, London, Special, pp. 65–79.
Anderson, E.M., 1905. The dynamics of faulting. Edinburgh Geological Society Transections 8, 387–402.
Anderson, E.M., 1942. The Dynamics of Faulting and Dyke Formation with Applications to Britain. Oliver and Boyd, Edinburgh, pp. 191.
Basa, A., Ahmed, F., Bhattacharyya, K., Roy, A., 2019. Evolution and characterization of fracture patterns: insights from multi-scale analysis of the Buxa dolomite in the Siang Valley, Arunachal Lesser Himalayan fold-thrust belt. J. Struct. Geol. 123, 54–66.
Bhakuni, S.S., Luirei, K., Kothyari, G.C., Imsong, W., 2017. Transverse tectonic structural elements across Himalayan mountain front, eastern Arunachal Himalaya, India: implication of superposed landform development on analysis of neotectonics. Geomorphology 282, 176–194.
Bhattacharya, S., Nandy, S., 2007. Geology of the Western Arunachal Himalaya in Parts of Tawang and west Kameng districts, Arunachal Pradesh. J. Geol. Soc.India 72, 199–207.
Bhattacharyya, K., Mitra, G., 2009. A new kinematic evolutionary model for the growth of a duplex-an example from Ranjit duplex, Sikkim Himalaya, India. Gondwana Res. 16, 697–715.
Bhattacharyya, K., Mitra, G., Kwon, S., 2015a. Geometry and kinematics of the Darjeeling–Sikkim Himalaya, India: implications for the evolution of the Himalayan fold-thrust belt. J. Asian Earth Sci. 113, 778–796.
Bhattacharyya, K., Dwivedi, H.V., Das, J.P., Damania, S., 2015b. Structural geometry, microstructuralandstrainanalysesofL-tectonites fromPaleoproterozoicorthogneiss: insights into local transport-parallel constrictional strain in the Sikkim Himalayan fold thrust belt. J. Asian Earth Sci. 107, 212–231.
Bhusan, S.K., Bindal, C.M., Aggarwal, R.K., 1991. Geology of bomdila group in Arunachal Pradesh. J. Himal. Geol. 2, 207–214.
Borgohain, D., Singh, J., 1999. Secondary recovery with simultaneous gas and water injectionin a Barail sandstone reservoir in Upper Assam. In: Proc. 3rd Int. Conf. And Exbn, Petrotech, 99, New Delhi, V, 257-260.
Bose, N., Mukherjee, S., 2019a. Field documentation and genesis of the back-structures from the Garhwal Lesser Himalaya. Uttarakhand, India. Tectonic implications. In: In: Sharma, Villa, I.M., Kumar, S. (Eds.), Crustal Architecture and Evolution of the Himalaya-Karakoram-Tibet Orogen, vol. 481. Geological Society of London Special Publications, pp. 111–125.
Bose, N., Mukherjee, S., 2019b. Field documentation and genesis of back-structures in ductile and brittle regimes from the foreland part of a collisional orogen: examples from the Darjeeling–Sikkim Lesser Himalaya, India. Int. J. Earth Sci. 108, 1333–1350.
Chakraborty, S., Mukul, M., 2019. New insights into the position and geometry of the main central thrust from Sikkim, eastern Himalaya. J. Geol. 127, 289–322.
Cloos, H., 1928. Zentralblatt fur Mineralogie and Palaeontology, vol. 1928, 609–621 B. Experimente zur inner Tektonik.
Dasgupta, A.B., Biswas, A.K., 2000. Geology of Assam. Geol. Soc. Ind. 170p.
Dasgupta, S., Mukhopadhyay, M., Nandy, D.R., 1987. Active transverse features in Central portion of the Himalaya. Tectonophysics 136, 255–264.
Dasgupta, S., Mukhopadhyay, B., Mukhopadhyay, M., 2013. Role of transverse tectonics in the Himalayan collision: further evidences from two contemporary earthquakes. J. Geol. Soc. India 81, 241–247.
De, R., Kayal, J.R., 2003. Seismotectonic model of the Sikkim Himalaya: constraint from microearthquake surveys. Bull. Seismol. Soc. Am. 93 (3), 1395–1400. https://doi.org/10.1785/0120020211.
De Sarkar, S., Mathew, G., Pande, K., Phukon, P., Singhvi, A.K., 2014. Drainage migration and out of sequence thrusting in Bhalukpong,Western Arunachal Himalaya, India. J. Geodyn. 81, 1–16.
DeCelles, P.G., Robinson, D.M., Zandt, G., 2002. Implications of shortening in the Himalayan fold-thrust belt for uplift of the Tibetan Plateau. Tectonics 21, 10–62.
Devi, R.K.M., Bhakuni, S.S., Bora, P.K., 2010. Tectonic implication of drainage set-up in the Sub-Himalaya: a case study from Papumpare district, Arunachal Himalaya, India. J. Geomorphology. https://doi.org/10.1016/j.geomorph.2010.11.010.
Ding, L., Zhong, D., Yin, A., Kapp, P., Harrison, M., 2001. Cenozoic structural and metamorphic evolution of the eastern Himalayan syntaxis (Namche Barwa). Earth Planet Sci.Lett 192, 423–438.
Duarah, B.P., Phukan, S., 2013. Understanding the tectonic behaviour of the Shillong plateau, India using remote sensing data. J. Geol. Soc. India 77, 105–112.
Dubey, A.K., 2014. Understanding an Orogenic Belt. Springer International, pp. 389p.
Dutta, D., Biswas, T., Mukherjee, S., 2019. Arc-parallel compression in the NW Himalaya: evidence from structural and palaeostress studies of brittle deformation from the clasts of the Upper Siwalik, Uttarakhand, India. Journal of Earth System Science 128, 125.
Gangopadhyay, P.K., Ray, S., 1980. Tectonic framework of the rangit window around Namchi, south Sikkim. Himal. Geol. 10, 338–353.
Ghosh, G.K., Basha, S.K., Salim, M., Kulshreshth, V.K., 2010. Integrated interpretation of seismic, gravity, magnetic andmagneto-telluric data in geologically complex thrust beltareas of Manabum, Arunachal Pradesh. J. Ind. Geophys. Union 14 (1), 1–14.
Godin, L., Harris, L.B., 2014. Tracking basement cross strike discontinuities in the Indian crust beneath the Himalayan orogen using gravity data-relationship to upper crustal faults. Geophys. J. Int. 198, 198–215.
Godin, L., La Roche, R.S., Waffle, S., Harris, L.B., 2019. Influence of inherited Indian basement faults on the evolution of the Himalayan orogen. In: In: Sharma, R., Villa, I., Kumar, S. (Eds.), Crustal Architecture and Evolution of the Himalaya-Karakoram-Tibet Orogen ume 481. Geological Society, London, Special, pp. 251–276.
Goswami, S., Bhowmik, S.K., Dasgupta, K., 2009. Petrology of a non-classical barrovian inverted metamorphic sequence from the western Arunachal Himalaya, India. J. Asian Earth Sci. 36, 390–406.
Goswami, T.K., Bhattacharyya, P., Bezbaruah, D., 2017. Mylonitic volcanics near Puging, Upper Siang district, Arunachal Pradesh: evidence of oblique-slip thrusting. J. Earth Syst. Sci. https://doi.org/10.1007/s12040-016-0728-4.
Goswami, T.K., Bezbaruah, D., Mukherjee, S., Sarmah, R.K., Jabeed, S., 2018. Structures and morphotectonic evolution of the frontal fold–thrust belt, Kameng river section, Arunachal Himalaya, India, Jour. Earth Sys. Sci 127, 88. https://doi.org/10.1007/

s12040-018-0984-6.
Handique, G.K., Bogohain, J.K., 1984. Subsurface structure and its role in the hydrocarbon entrapment in parts of upper Assam oil field region. Proc. Vol. Seminar on Recent Advances on the Study of the Cainozoic Geology of the North Eastern Region of India. Dibrugarh University, pp. 66–88 March 28-31.
Haproff, P.J., Zuza, A.V., Yin, A., Harrison, T.M., Manning, C.E., Dubey, C.S., Ding Lin, Wu, C., Chen, J., 2019. Geologic framework of the northern indo-burma ranges and lateral correlation of Himalayan-Tibetan lithologic units across the eastern Himalayan syntaxis. Geosphere 15, 1–26.
Hazarika, P., Ravi Kumar, M., Srijayanthi, G., Soloman Raju, P., Purnachandra Rao, N., Srinagesh, D., 2010. Transverse tectonics in the Sikkim Himalaya; evidence from seismicity and focal mechanism. Bull Seismol Soc Am 100, 1816–1822.
Holdsworth, R.E., Tavarnelli, E., Clegg, P., Pinheiro, R.V.L., Jones, R.R., McCaffrey, K.J., W, 2002. Domainal deformation patterns and strain partitioning during transpression: anexample from the Southern Uplands terrane, Scotland. J. Geol. Soc. Lond. 159, 401–415.
Hossain, Md S., Khan, Md S.H., Chowdhury, K.R., Abdullah, R., 2019. Synthesis of the tectonic and structural elements of the Bengal basin and surroundings. In: Mukherjee, S. (Ed.), Tectonics and Structural Geology: Indian Context. Springer, 978-3-319-99340-9, pp. 135–218.
Hu, X., Garzanti, E., Wang, J., Huang, W., An, W., Webb, A., 2016. The Timing of India-Asia collision onset–facts, theories, controversies. Earth Sci. Rev. 160, 264–299.
Huyghe, P., Galy, A., Mugnier, J.L., France-Lanord, C., 2001. Propagation of the thrust system and erosion in the Lesser Himalaya: geochemical and sedimentological evidence. Geology 29, 1007–1010.
Jayangondaperumal, R., Thakur, V.C., Joevivek, V., Rao, P.S., Gupta, A.K., 2018. Active Tectonics of Kumaun and Garhwal Himalaya. Springer Natural Hazards978-981-10-8243-6.
Jodha, B.S., 1991. Geology of the Area Around Garu-Gensi. West Siang District, Arunachal Pradesh: GSI, Unpub Prog. report, FS-1991-92.mb.
Jones, R.R., Holdsworth, R.E., Clegg, P., McCaffrey, K., Tavarnelli, E., 2004. Inclined transpression. J. Struct. Geol. 26, 1531–1548.
Kayal, J.R., 2001. Microearthquake activity in some parts of Himalaya and the tectonic model. Tctonophysics 339, 331–351.
Kayal, J.R., De, R., Chakraborty, P., 1993. Microearthquakes at the main boundary thrust in Eastern Himalaya and the present-day tectonic model. Tectorrophysics 218, 375–381.
Kayal, J.R., Arefiev, S.S., Baruah, S., Tatevossian, R., Gogoi, N., Sanoujam, M., Gautam, J.L., Hazarika, D., Borah, D., 2010. The 2009 Bhutan and Assam felt earthquakes (Mw6.3 and 5.1) at the Kopili fault in the northeast Himalaya region. Geomatics, Nat. Hazards Risk 1, 273–281.
Kesari, G.K., 2010. Geology and Mineral Resources of Arunachal Pradesh, vol. 30 GSI, Misc Pub IV, I.
Kumar, G., 1997. Geology of Arunachal Pradesh. Geol. Soc. Ind. Bangalore, pp. 217p.
Kumar, R., Singh, T., 1974. Lithostratigraphy of southern parts of Siang district, Arunachal Pradesh. Himal. Geol. 4, 648–656.
Mandal, K., Dasgupta, R., 2013. Upper Assam Basin and its Basinal Depositional History SPG 10th Biennial International Conference and Exposition. pp. 1–7 Kochi.
Martin, A.J., 2017. A review of Himalayan stratigraphy, magmatism, and structure. Gondwana Res. 49, 42–80.
Matin, A., Mazumdar, S., 2009. Deformation mechanisms in the frontal lesser Himalayan duplex in Sikkim Himalaya, India. J. Earth Syst. Sci. 118, 379–390.
Matin, M., Mukul, M., 2010. Phases of deformation from cross-cutting structural relationships in external thrust sheets: insights from small-scale structures in the Ramgarh thrust sheet, Darjiling Himalaya, West Bengal. Curr. Sci. 99, 1369–1377.
McQuarrie, N., Robinson, D., Long, S., Tobagay, T., Grujic, D., Gehrels, G., Ducea, M., 2008. Preliminary stratigraphic and structural architecture of Bhutan: implications for along strike architecture of the Himalayan system. Earth Planet. Sci. Lett. 272, 105–117.
Mishra, D.K., 2009. Litho-tectonic sequence and their regional correlation along the Lohit and Dibang valleys, eastern Arunachal Pradesh. J. Geol. Soc. India 73, 213–219.
Mitra, G., Bhattacharyya, K., 2011. The use of cleavage-bedding relations and mesoscopic structures in interpreting complex duplex geometries in fold-thrust belts: examples from the Rangit duplex, Sikkim Himalaya. Himal. Geol. 32, 25–42.
Mukherjee, S., 2011. Mineral Fish: their morphological classification, usefulness as shear sense indicators and genesis. Int. J. Earth Sci. 100, 1303–1314.
Mukherjee, S., 2014. Review of flanking structures in meso- and micro-scales. Geol. Mag. 151, 957–974.
Mukherjee, S., 2015. A review on out-of-sequence deformation in the Himalaya. In: In: Mukherjee, S., Carosi, R., van der Beek, P., Mukherjee, B.K., Robinson, D. (Eds.), Tectonics of the Himalaya, vol. 412. Geological Society, London. Special Publications, pp. 67–109.
Mukherjee, S., 2017. Review on symmetric structures in ductile shear zones. Int. J. Earth Sci. 106, 1453–1468.
Mukherjee, S., Punekar, J.N., Mahadani, T., Mukherjee, R., 2016. In: Mukherjee, S., Mulchrone, K.F. (Eds.), Intrafolial Folds: Review and Examples from Western Indian Higher Himalaya, Ductile Shear Zones: from Micro- to Macro-Scales. John Wiley & Sons, pp. 182–205.
Mukhopadhyay, M., 1984. Seismotectonics of transverse linea- ments in the eastern Himalaya and its fore-deep. Tectonophysics 109, 227–240.
Mukul, M., 2000. The geometry and kinematics of the Main Boundary Thrust and related neotectonics in the Darjiling Himalayan fold-and-thrust belt, West Bengal, India. J. Struct. Geol. 22, 1261–1283.
Mullick, B.B., Basu Chowdhury, S., 1966. Geology of Parts of Siang District, NEFA. Geol. Surv. Ind. Progress Report FS 1966-67 (unpublished).
Murty, K.N., 1983. Geology and hydrocarbon prospects of Assam shelf-Recent advances and present statutes. Petroleum Asia Journal 6, 1–14.
Najman, Y., Jenks, D., Godin, L., Boudagher-Fadel, M., Millar, I., Garzanti, E., Bracciali, L., 2017. The Tethyan Himalayan detrital record shows that India–Asia terminal collision occurred by 54 Ma in the Western Himalaya. Earth Planet. Sci. Lett. 459, 301–310.
Nakata, T., 1989. Active faults of the Himalaya of India and Nepal. Geol. Soc. Am. Spec. Pap. 232, 243–264.
Nandy, D.R., 1980. Tectonic patterns in northeastern India. Ind. 3. Earth Sci. 7, 103–107.
Ningthoujam, P.S., Dubey, C.S., Lolee, L.K., Shukla, D.P., Naorem, S.S., Singh, S.K., 2015. Tectonic studies and crustal shortening across easternmost Arunachal Himalaya. J. Asian Earth Sci. 111, 339–349.
Pandey, A., Singh, I., Mishra, R.L., Rao, P.S., Srivastava, H.B., Jayangondaperumal, R., 2018. Active tectonics in the Assam seismic gap between themeizoseismal zone of AD 1934 and 1950 earthquakes along eastern Himalayan front, India. J. Earth Syst. Sci. 127, 66.
Pauri, C. and Bhattacharyya, K. 2018 Duplex and along-strike structural variation: a case study from Sikkim Himalayan fold thrust belt, J. Struct. Geol., 113, 62-75.
Paudel, L., Arita, K., 2000. Tectonic and polymetamorphic history of the Lesser Himalaya in central Nepal. J. Asian Earth Sci. 18, 561–584.
Pearson, O.N., DeCelles, P.G., 2005. Structural geology and regional tectonic significance of the Ramgarh thrust, Himalayan fold-thrust belt of Nepal. Tectonics 24, TC4008.
Prasad, B.R., Rao, V., 2006. Deep seismic reflection study over the Vindhyans of Rajasthan: implications for geophysical setting of the basin. J. Earth Syst. Sci. 115, 135–147.
Pratap, M., Kutty, A., Patra, S.K., 1997. The modified geological model for Charali Field, Assam by reservoir simulation study. Proc. 2nd Int. Petrol. Conf. And Exbn, Petrotech 97, 419–428 New Delhi.
Raiverman, V., Srivastava, A.K., Prasad, D.N., 1994. Structural Style in Northwestern Himalayan foothills. J. Himal. Geol. 15, 263–280.
Ramsay, J.G., 1967. Folding and Fracturing of Rocks. McGraw Hill, New York, pp. 568p.
Rao, A.R., 1983. Geology and hydrocarbon potential of a part of Assam-Arakan Basin and its adjacent region. Petrol. Asia. Jr. 6 (4), 127–158.
Ray, S.K., 1995. Lateral variation in geometry of thrust planes and its significance, as studied in the shumar allochthon, lesser Himalayas, Eastern Bhutan. Tectonophysics 249, 125–139.
Ray, S.K., Bandyopadhyay, B.K., Razdan, R.K., 1989. Tectonics of a part of the Shumar allochthon. Tectonophysics, vol. 169, 51–58 Eastern Bhutan.
Roy, A.B., Chatterjee, A., 2015. Tectonic framework and evolutionary history of Bengal Basin in the Indian subcontinent. Curr. Sci. 109 (2), 271–279.
Roy Chowhury, J., 1978. Geology of the Area Around Abor Hills, Garu, Gensi, Tatamori, Daporjo, Yinkiong, Siang and Subansiri Districts, and Around Bairabkund, Khellong and Tipi, Kameng District, Arunachal Pradesh, Geol. Surv. India, Progress Report. (Unpublished).
Saha, D., 2013. Lesser Himalayan sequences in Eastern Himalaya and their deformation:implications for Paleoproterozoic tectonic activity along the northern margin of India. Geosci. Front. 289–304.
Saha, D., Sengupta, D., Das, S., 2011. Along strike variation in the Himalayan orogen and its expression along major intracontinental thrusts – the case of MCT in Sikkim and Arunachal Pradesh, India. In: In: Tewari, R.P. (Ed.), Geodynamics, Sedimentation and Biotic Response in the Context of India-Asia Collision, vol. 77. Memoir of the Geological Society of India, pp. 1–18.
Sahoo, M., Gogoi, K.D., 2011a. Structural Style and its Implication on Petroleum Systems of North Assam Shelf, Upper Assam Basin. GEO- India, India, pp. 1–16 Extended Abstract.
Sahoo, M., Gogoi, K.D., 2011b. Structural styles and its implication on petroleum systems of north Assam shelf, upper Assam basin, India. In: 2nd South Asian Geosciences Conference and Exhibition GEO India2011, 12–14 Jan, New Delhi India.
Sarma, J.N., Sharma, S., 2018. Neotectonic activity of the Bomdila Fault in northeastern India from geomorphological evidences using remote sensing and GIS. J. Earth Syst. Sci. 127, 113.
Sarma, K.P., Bhattacharya, S., Nandy, S., Konwar, P., 2014. Structure, stratigraphy and magnetic succeptibility of Bomdila gneiss, western Arunachal Himalaya, India, Jour. Geol.Soc. Ind. 88, 544–554.
Sarma, K.P., Sharma, R., Majumdar, N., 2017. Geological framework of western Arunachal Himalaya and eastern Arunachal Himalaya-are they identical?Some observations. Am Int. Jour. Res. Sc. Eng. Math. 17–316, 51–58.
Sarmah, R.K., 2013. Spatio-temporal variation in the quality of Oligocene coals of the Tikak parbar formation, Makum coal filed, north eastern India. Ind. Strm. Res. Jour. 3 (4), 34–39.
Schelling, D., Arita, K., 1991. Thrust tectonics, crustal shortening, and the structure of the far-eastern Nepal Himalaya. Tectonics 10, 851–862.
Shah, J., Srivastava, D.C., Joshi, S., 2012. Sinistral transpression along the main boundary thrust in Amritpur area, southeastern Kumaun Himalaya. Tectonophysics 532–535, 258–270.
Singh, T., 1981. Age and faunal affinity of the Garu formation. Areunachal Pradesh, Himalayan Geology 11, 271–286.
Singh, S., 1993. Geology and tectonics of the eastern syntaxial bend, Arunachal Himalaya. J. Himal. Geol. 4, 149–163.
Singh, S., Chowdhury, P.K., 1990. An outline of the geological framework of the Arunachal, Himalaya. J. Himal. Geol. 1, 189–197.
Singh, R.K.B., Gururajan, N.S., 2011. Microstructures in quartz and feldspars of the Bomdila gneiss from western Arunachal Himalaya, northeast India: implications for the geotectonic evolution of the Bomdila mylonitic zone. J. Asian Earth Sci. 42, 1163–1178.
Singh, S., Malhotra, G., Gupta, P., Misri, J.L., 1983. Geology of east and west Siang districts, Arunachal Pradesh, north of Gondwana belt, unpub. Prog. Rep. Geol. Surv.

Ind., FS 1982-83.
Srikantia, S.V., 1989. Main BoundaryFault of the Himalaya- A concept that is no longer valid. 22. Punjab University, Chandigarh, pp. 1–18 Bull. Ind. Geol. Assoc.
Srivastava, P., Misra, D.K., 2008. Morpho-sedimentary records of active tectonics atthe Kameng River exit, NE Himalaya. Geomorphology 96, 187–198.
Srivastava, P., Mitra, G., 1994. Thrust geometries and deep structure of the outer and lesser Himalaya, Kumaon and Garhwal (India): implications for evolution of the Himalayan fold-and-thrust belt. Tectonics 13, 89–109.
Srivastava, H.B., Srivastava, V., Srivastava, R.K., Singh, C.K., 2011. Structural analyses of the crystalline rocks between dirang and Tawang, west Kameng district, Arunachal Himalaya. J. Geol. Soc. India 78, 45–56.
Srivastava, H.N., Verma, M., Bansal, B.K., Sutar, A.K., 2013. Discriminatory characteristics of seismic gaps in Himalaya. Geomatics, Nat. Hazards Risk 6, 224–242.
Sylvester, A.G., 1988. Strike-slip faults. Geol. Soc. Am 100, 1666–1703.
Tavani, S., Storti, F., Lacombe, O., Corradetti, A., Muñoz, J.A., Mazzoli, S., 2015. A review of deformation pattern templates in foreland basin systems and fold-and-thrust belts: implications for the state of stress in the frontal regions of thrust wedges. Earth Sci. Rev. 141, 82–104.
Tchalenco, J.S., 1970. Similarities between shear zones of different magnitudes. Geol. Soc. Am. Bull. 81, 1625–1640.
Tripathi, C., Roy Chowdhury, J., 1983. Gondwana of Arunachal Himalaya. Him.Geol 11, 73–89.
Valdiya, K.S., 1980a. The Two Intracrustal Boundary Thrusts of the Himalaya, vol. 66. Tectonophys, pp. 323–348.
Valdiya, K.S., 2001. Reactivation of terrane-defining boundary thrusts in central sector of the Himalaya: Implications. Curr. Sci. 81, 1418–1431.
Valdiya, K.S., Rana, R.S., Sharma, P.K., Dey, P., 1992. Active Himalayan frontal fault, main boundary thrust and Ramgarh thrust in southern Kumaun. J. Geol. Soc. India 40, 509–528.
Wu, C., Nelson, K.D., Wortman, G., Samson, S.D., Yue, Y., Li, J., Kidd, W.S.F., Edwards, M.A., 1998. Yadong cross structure in south Tibetan detachment in east central Himalaya (89°- 90° E). Tectonics 17, 28–45.
Yin, A., 2006. Cenozoic tectonic evolution in the Himalayan orogen as constrained by the along-strike variation of the structural geometry, exhumation history, and foreland sedimentation. Earth Sci. Rev. 76, 1–13.
Yin, A., Taylor, M.H., 2011. Mechanics of V-shaped conjugate strike-slip faults and the continuum mode of continental deformation. Geol. Soc. Am. Bull. 123, 1798–1821.
Yin, A., Dubey, C.S., Kelty, T.K., Webb, A.A.G., Harrison, T.M., Chou, C.Y., Célérier, Julian, 2010. Geologic correlation of the Himalayan orogen and Indian craton: Part 2. Structural geology, geochronology and tectonic evolution of the Eastern Himalaya GSA Bulletin 22, 360–395.